

R-2578-FF

HOW TO ASSESS THE SURVIVABILITY OF U.S. ICBMs: APPENDIXES

Bruce W. Bennett

SUPPORTED BY A GRANT FROM
THE FORD FOUNDATION

A SERIES IN INTERNATIONAL
SECURITY AND ARMS CONTROL

JUNE 1980



This publication was supported by Grant No. 790-0061 from
The Ford Foundation.

Library of Congress Cataloging in Publication Data

Bennett, Bruce W
How to assess the survivability of U. S.
ICBMs.

([Report] - The Rand Corporation ; R-2577-FF-R-
2578-FF)

Based on the author's thesis, Rand Graduate
Institute.

Vol. 2: Appendixes.

Bibliography: v. , p.

1. Intercontinental ballistic missile bases--
United States. 2. Intercontinental ballistic
missiles. 3. Atomic warfare. I. Ford
Foundation. II. Title. III. Title:
Survivability of U.S. ICBMs. IV. Series:
Rand Corporation. Rand report ; R-2577-FF-R-2578-
FF.

AS36.R3 R-2577-2578 [UG733] 081s
ISBN 0-8330-0241-4 (v. 1) [358'.1754'0973]
ISBN 0-8330-0242-2 (v. 2) 80-18113

The Rand Publication Series: The Report is the principal
publication documenting and transmitting Rand's major
research findings and final research results. The Rand Note
reports other outputs of sponsored research for general
distribution. Publications of The Rand Corporation do not
necessarily reflect the opinions or policies of the sponsors of
Rand research.

Published by The Rand Corporation

R-2578-FF

HOW TO ASSESS THE SURVIVABILITY OF U.S. ICBMs: APPENDIXES

Bruce W. Bennett

SUPPORTED BY A GRANT FROM
THE FORD FOUNDATION

A SERIES IN INTERNATIONAL
SECURITY AND ARMS CONTROL

JUNE 1980



PREFACE

In late 1978, The Ford Foundation provided grants to The Rand Corporation and several university centers for research and training in international security and arms control. At Rand, the grant is supporting a diverse program. In the Rand Graduate Institute, which offers a doctorate in policy analysis, the grant is contributing to student fellowships for dissertation preparation, curriculum development, workshops and tutorials, and a series of visiting lecturers. In Rand's National Security Research Division, the Ford-sponsored projects are designed to extend beyond the immediate needs of government sponsors of research by investigating long-term or emerging problems and by developing and assessing new research methodologies. The grant also is being used to fund the publication of relevant sponsored research that would otherwise not be disseminated to the general public.

All research products are being made available to as wide an audience as possible through publication as unclassified Rand reports or notes, or in journals. The Rand documents may be obtained directly or may be found in the more than 330 libraries in the United States and 35 other countries that maintain collections of Rand publications.

This report is composed of six technical appendixes to companion report R-2577-FF, *How To Assess the Survivability of U.S. ICBMs*. These appendixes provide substantive background on some aspects of ICBM survivability, supporting the principal report's development of a methodology for assessing ICBM survivability. A summary of this methodology is contained in R-2577-FF. The technical appendixes should be of interest to strategic analysts and others who desire to delve into this subject beyond the material presented in the principal report.

ACKNOWLEDGMENTS

The author is grateful for the helpful suggestions and guidance provided by his dissertation committee: James Foster and William Hoehn of Rand, and Henry Rowen of Stanford University. Victor Jackson and Theodore Garber of Rand also provided important assistance in reviewing this report after it had passed the dissertation phase. Full responsibility for the results and information presented remains, of course, with the author.

GLOSSARY AND SYMBOLS

A_{vn}	Overpressure pulse duration correction for the VN
B_h	Systematic error in height of burst caused by systematic impact bias
Bias	Systematic bias error (the distance between the target and the mean point of impact)
C	Relative confidence that a missile is in a high probability rather than a low probability aimpoint
CEP	Circular error probable (distance from mean point of impact within which 50 percent of many shots should fall)
D	Number of shelters per missile in an MPS system
DIA	Defense Intelligence Agency
E	Fraction of an MPS system assumed to be "empty" of missiles
F	Percentage of warheads surviving fratricide
$F(\cdot)$	Cumulative distribution function for distance from target to impact points
$G(\cdot)$	Cumulative distribution function for warhead closest to target
h	Overpressure produced at the target (ground distance x from detonation)
h_o	Overpressure required to destroy a target (the target hardness)
H	Fraction of MPS system in high probability subset
HOB	Height of burst of the warhead detonation
HOB _o	Intended height of burst
K	K-factor (a measure of overpressure pulse duration sensitivity)
kt	Kilotons (warhead yield, thousands of tons TNT equivalent)
L	Fraction of MPS system in low probability subset
Ln	Natural logarithm
Log	Logarithm base 10
LR	Lethal radius of a warhead against a particular target type
LR ₅₀	Lethal radius at which 50 percent of all targets would be destroyed
Mt	Metatons (warhead yield, millions of tons TNT equivalent)
MPS	Multiple protective shelters

$N(\mu, \sigma^2)$	Normal distribution, with mean μ and variance σ^2
n	Number of warheads attacking each silo or aimpoint
N	Number of defending missiles in an MPS system
N_H	Number of defending missiles actually contained in high probability aimpoints
N_L	Number of defending missiles actually contained in low probability aimpoints
n mi	Nautical miles
N_s	Number of missiles surviving an attack
P_{50}	Overpressure required to destroy a target with 50 percent probability (the basis of a VN)
P_H	Probability that a high probability shelter contains a missile
P_L	Probability that a low probability shelter contains a missile
PA	Probability a warhead arrives and detonates on target
PD	Kill probability desired against an MPS system
PK	Multiple-shot kill probability
PK_1	PK for one warhead
PK_2	PK for two warheads
psi	Overpressure measure (pounds per square inch)
PT	Net kill probability against an MPS system
PT_H	PT against high probability shelters
PT_L	PT against low probability shelters
Q	Ratio of attack size (TN) against the MPS system to the total number of shelters (DN)
SSPK	Kill probability against a target of a single arriving, detonating warhead
SSPS	Survival probability of a target to a single arriving, detonating warhead (1-SSPK)
T	Number of tests made of a parameter's value
TN	Total number of warheads used in an attack
VN	Vulnerability number representation for target hardness
VN_o	VN before adjustment for sensitivity to overpressure pulse duration
W	Variable calculated by iteration to give the value for A_{vn}
WR	Weapon radius of a warhead against a particular target type
x	Ground distance from warhead detonation
x_o	Ground distance between detonation and location receiving overpressure h_o
Y	Warhead yield (total energy released by the warhead explosion, in TNT equivalents)
Z	Scaled distance (thousands of feet)

α	Cumulative probability of a particular statistical test
β	Function of the damage sigma (σ_d), used in SSPK
β_r	Reentry angle of an incoming warhead
θ	Power used to "scale" yield (normally one-third)
λ	Slope of log-log relationship between overpressure versus ground range ($\lambda = \phi/\beta$)
σ	Standard deviation (square root of variance)
σ_c	Standard deviation of crossrange impact errors
σ_D	Standard deviation of downrange impact errors
σ_d	Damage sigma (of lognormal damage distribution)
σ_h	Standard deviation of height of burst variability
σ_t	Timing variation for each warhead impacting a given silo
σ_{WR}	Standard deviation of weapon radius uncertainty
σ_θ	Standard deviation of θ (yield scaling factor)
ϕ	Function used to determine SSPK based on overpressure ($\phi = 0.297$)
χ^2	Chi square statistic

CONTENTS

PREFACE	iii
ACKNOWLEDGMENTS	v
GLOSSARY AND SYMBOLS	vii
FIGURES	xiii
TABLES	xv
Appendix	
A. THE EFFECT OF RANDOM VARIATIONS	1
Random Variations Around "Expected" Outcomes ..	1
Types of Random Variations.	2
B. SOME NOTES ON LETHAL RADII, SSPK, OVERPRESSURE, AND VULNERABILITY NUMBERS	6
The Lethal Radius of the Traditional Model	6
Comparing SSPK Values Across Models	7
Overpressure and Vulnerability Numbers	9
C. COMPLICATIONS IN THE SSPK RELATIONSHIPS	11
Modeling Warhead Destructiveness	11
Accuracy Complications	19
Height of Burst Uncertainty and Accuracy	24
D. DERIVATION OF THE FORMULA FOR THE IMPACT DISTRIBUTION OF THE "CLOSEST" WARHEAD	32
E. PHYSICALLY MODELING FRATRICIDE	34
The Physics of Fratricide	34
A Sample Calculation of Fratricide in the Early Window	36
Problems with the Second Window	39
Trying to Overcome Fratricide	41
F. CONFIDENCE IN OVERCOMING MPS DECEPTION ...	43
The Basic Formulation	43
Attacking the MPS System	45
The Limits of Confidence	53
Conclusions	55
BIBLIOGRAPHY	57

FIGURES

A.1	95% Confidence Interval for Actual SSPK Assuming Binomial Variability Around Expected SSPK	2
A.2	Effect of Target-to-Target Impact Variability on PK for Multiple Warhead Attacks	5
B.1	Relationship Between SSPK and the Ratio of Weapon Radius to CEP for Two Damage Functions	8
C.1	Ground Range for Various Overpressure Levels for a 1-kt Groundburst	12
C.2	Ground Range for Various Overpressure Levels for a 1-kt Optimal Airburst	13
C.3	Overpressure Required for a Given SSPK Using the DIA Damage Function	17
C.4	Ground Range for High Overpressure Levels for a 1-kt Airburst	18
C.5	Comparison of True SSPK to SSPK Based on CEP Approximations	21
C.6	Alternative Distributions for Downrange or Crossrange Miss Distance	22
C.7	Comparison of Two Impact Distributions With Equal CEPs Calculated from Standard Deviations	23
C.8	Airburst Schematic Diagram	25
C.9	Effect of Random Uncertainty in HOB on CEP for Differing Reentry Angles, $\sigma_D = \sigma_C$	27
C.10	Effect of Random Uncertainty in HOB on CEP for Differing Ratios of $\sigma_D:\sigma_C$, $\beta = 22^\circ$	27
C.11	Effect of Height of Burst Uncertainty on Preference for Airbursting	29
C.12	Degradation of Average SSPK Due to Effect of Height of Burst Uncertainty on Weapon Radius	30
E.1	Effect of Fratricide on a Warhead Timed To Arrive in the First Window After a Previous Nuclear Detonation on the Same Target	37
E.2	Probability That Warheads Will Survive Fratricide and Detonate If Four Warheads Are Assigned to a Target With Various Delays	38
F.1	Confidence Required To Guarantee That Only a Given Number of Missiles Are in Low Probability Shelters	47

F.2	Areas of "Deception Space" Where the Different Formulations Apply	52
F.3	Breakdown in Deception Required for Specific Number of Surviving Missiles (N_s)	53
F.4	Breakdown in Deception Required for Different Force Sizes To Reduce the Number of Surviving Missiles to 60.	54

TABLES

A.1	Examples of Different Kinds of Variability	3
C.1	σ_d Versus ϕ for Varying Pressure/Distance Slopes (λ) ..	16
F.1	Equations for Determining the Number of Surviving Shelters	49
F.2	Nominal Formulation of Surviving Shelters	51

Appendix A

THE EFFECT OF RANDOM VARIATIONS

Although some aspects of random variations are discussed in the main volume of this report, R-2577-FF, many are not because they are generally more complicated (especially in terms of calculation) and less significant than the effect of uncertainty in the mean value of a parameter. This appendix will try to parameterize some of the various aspects of random variations to show how much difference they can make. In almost all cases, these effects must be added to the uncertainty effects shown in the text, making the true outcomes even more uncertain than shown in R-2577-FF.

RANDOM VARIATIONS AROUND "EXPECTED" OUTCOMES

As noted in Sec. III of R-2577-FF, all of the calculations in the text ignore random variations in calculating the impact of uncertain parameters. That is, in each Monte Carlo simulation of the uncertain parameters, an "expected" kill probability is found based upon the simulated parameter values, rather than going one step further and determining, on the basis of that probability, how many silos out of 1000 would be killed by warheads that have that *expected* kill probability in an actual laydown. By comparison, even with a fair coin that has a 50 percent *expected* probability of heads, there is some chance that after two flips, I would observe zero percent heads. Similarly, even if the *expected* kill probability of a warhead *really* is 90 percent, 1000 warheads arriving on different targets could well damage only 85 percent of those targets, or even 95 percent of them, depending on where the warheads actually land and on the other variabilities associated with the various parameters. Thus, even if the Soviets knew *exactly* the mean value of all of their parameters, there is still some "luck-of-the-draw" with which they would have to reckon.

In order to examine the potential impact of random variations, Fig. A.1 shows a 95 percent confidence interval for the single-shot kill probability (SSPK) of 1000 warheads, assuming that the random varia-

tions in SSPK are binomially distributed.¹ To the extent that this assumed distribution is correct, the effect of random variation in SSPK is quite small and adds only a very small amount to the uncertainty in most of the assessments in the text.

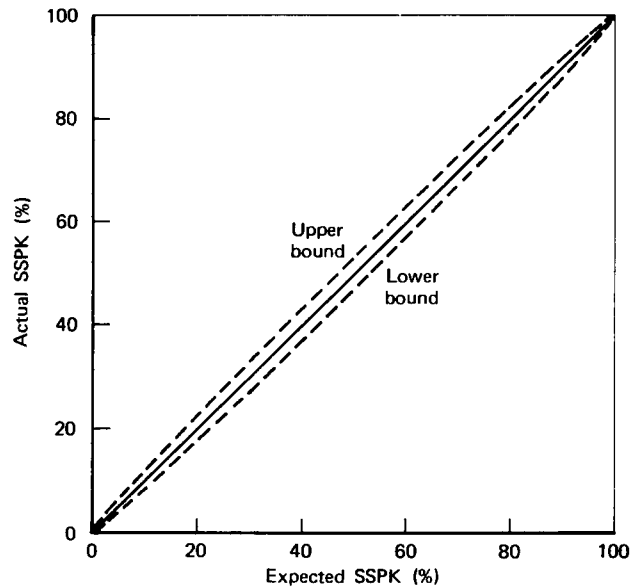


Fig. A.1—95% confidence interval for actual SSPK assuming binomial variability around expected SSPK

TYPES OF RANDOM VARIATIONS

In an attack on U.S. silos by Soviet MIRVed missiles, there are three kinds of random variations that should be differentiated. The first is the variability of each warhead (e.g., variations in the actual yield of the detonation). The second is the variability of each missile carrying the MIRVs (e.g., variations in launch versus launch failure).

¹Monte Carlo simulations of impact variability indicate that the resulting variations in SSPK are not exactly binomially distributed, and would produce an SSPK confidence interval for this number of warheads that would be somewhat smaller than the interval shown in Fig. A.1. However, other random variations would tend to increase the interval at least somewhat.

The third is the variability of each target (e.g., variations in actual hardness). The first and third kinds of variability have been referred to as "weapon-to-weapon" (actually, "warhead-to-warhead") and "target-to-target" variability, respectively. Table A.1 describes some examples of each, and indicates where in the text they are discussed in more detail.

Table A.1
EXAMPLES OF DIFFERENT KINDS OF VARIABILITY

Type of Variability	Example	Location of Discussion
Weapon-to-weapon	Height of burst errors	Height of burst uncertainty and accuracy, App. C
	Actual impact points	Figure A.1
Missile-to-missile	Dependent reliability	Arrival probability, Sec. IV
	Impact points	Figure A.2
Target-to-target	Target hardness	Modeling warhead destructiveness, App. C
	Altitude misestimation	Height of burst uncertainty and accuracy, App. C

Even with today's modern computers, it is extremely time consuming to take account of random variations in aggregate calculations around each of several hundred Monte Carlo samples used in assessing mean value uncertainty. Therefore, although many examples of variability are discussed herein, they are normally excluded from the uncertainty calculations (though in some cases, as with the damage sigma formulation of hardness variations, the biasing effect of the variation is accounted for, as shown in Fig. 3 of the main text). In most cases, the effect of these variations is relatively insignificant compared to the uncertainties evaluated; however, their exclusion does lead to an underestimate of the full range of uncertainties. Further,

especially when the calculations tend to show very high kill probabilities, the exclusion of variabilities tends to cause a net bias toward higher kill probabilities; thus, were all variabilities included, the average kill probabilities would be expected to drop somewhat.

There is perhaps no better example of this net bias than in the weapon inaccuracy variability. At one extreme, all warheads from the same missile could land in a totally uncorrelated pattern (no inaccuracy until after separation from the MIRV bus). At the other extreme, all inaccuracy could be due to errors before warhead separation, such that if two or more warheads from the same missile are fired at the same target, they would all land in the same place (their impact is completely correlated), as opposed to randomly dispersed (independently) around the target (as is usually assumed). In this latter case, an accurate missile would put all of its warheads right on the target, whereas an inaccurate one would miss with every shot. The effect of inaccuracy from weapon-to-weapon variability compared with missile-to-missile variability is shown in Fig. A.2 for two values of circular error probable (CEP). If the impact points are correlated, a second or subsequent warhead does not add much to the kill probability (PK), degrading the PK from the standard, uncorrelated damage outcome. This figure shows that for a 900 ft CEP, this degradation can be substantial. The exclusion of this kind of random variation thus tends to bias the kill probability on the high side; the extent of the bias is somewhat difficult to estimate because impacts are neither perfectly correlated nor uncorrelated.

It is important to note that the effect of missile-to-missile random variations of this sort can be largely offset by cross-targeting. As discussed in the subsection in R-2577-FF on arrival probability, warheads arriving at a target from the same booster are at least somewhat dependent on each other, whereas warheads from different boosters would be independent in their effects on any given target. Unfortunately, as discussed in App. E, cross-targeting makes timing of warhead impact more difficult, potentially increasing fratricide. Therefore, the reliability and impact degradations caused by booster errors must be evaluated against timing problems to assess whether or not cross-targeting is advantageous. It is beyond the scope of this analysis to synthesize the assessment of these individual errors.

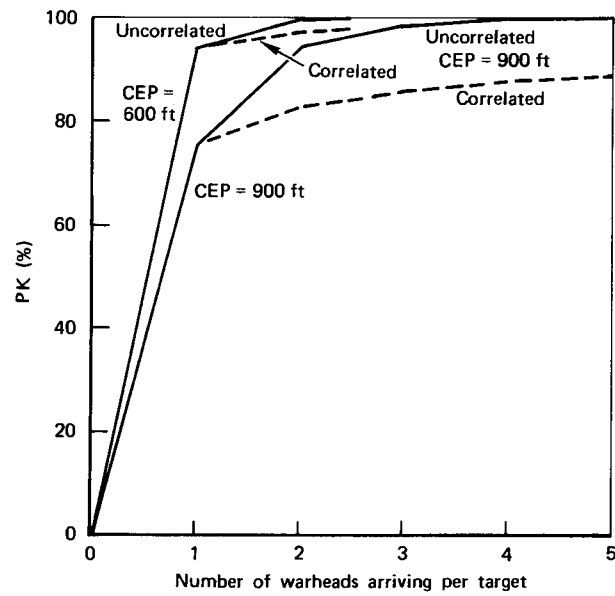


Fig. A.2—Effect of target-to-target impact variability on PK for multiple warhead attacks

Appendix B

SOME NOTES ON LETHAL RADII, SSPK, OVERPRESSURE, AND VULNERABILITY NUMBERS

THE LETHAL RADIUS OF THE TRADITIONAL MODEL

The relationship between overpressure and the distance at which that overpressure is created for a ground burst can be expressed as¹

$$h = 3.3 \cdot \frac{Y}{x^3} + 6.96 \cdot \left(\frac{Y}{x^3}\right)^{1/2}$$

where h is the overpressure in psi, Y is the yield in kt, and x is the distance in thousands of feet. If we define the variable Z to be the scaled distance, in thousands of feet,

$$Z = \frac{x}{Y^{1/3}}$$

then the above formula simplifies to

$$h = 3.3 \cdot Z^{-3} + 6.96 \cdot Z^{-3/2}$$

Multiplying through by Z cubed and rearranging the terms gives

$$h \cdot Z^3 - 6.96 \cdot Z^{3/2} - 3.3 = 0$$

Solving the quadratic equation for $Z^{3/2}$ produces

$$Z^{3/2} = \frac{6.96 \pm \sqrt{48.4 + 13.2 \cdot h}}{2 \cdot h}$$

¹Kosta Tsipis, *Nuclear Explosion Effects on Missile Silos*, Center for International Studies, Massachusetts Institute of Technology, February 1979, p. 20, converted to kilotons here. Note that Tsipis gives a value comparable to 6.07 rather than 6.96. However, for lower overpressure values, 6.96 comes much closer to matching the data in his figures and in other sources, as argued in App. C.

Since Z must be positive, Z can be expressed as

$$Z = \left(\frac{3.48 + \sqrt{12.1 + 3.3 \cdot h}}{h} \right)^{2/3}$$

Solving for x, in thousands of feet, gives

$$x = Y^{1/3} \cdot \left(\frac{3.48 + \sqrt{12.1 + 3.3 \cdot h}}{h} \right)^{2/3}$$

*The Effects of Nuclear Weapons*² values for h and x in Fig. C.1 match fairly closely those calculated with this equation. Note that x is the lethal radius (LR) required to determine SSPK in the traditional model.

COMPARING SSPK VALUES ACROSS MODELS

There are two ways in which the SSPK of the traditional model can differ from that of the vulnerability number system for the same threat parameters. First, the damage sigmas of the two procedures differ. Second, the two procedures use different formulas to obtain their lethal weapon radius. For targets of the hardness of ICBM silos, both of these differences work in the same direction, causing the traditional model to have a higher SSPK.

To examine these differences, it is necessary to show how the basic data in each system relate to each other. According to the Defense Intelligence Agency (DIA), the overpressure required to destroy the target with 50 percent probability (p_{50}) and the VN are related by

$$p_{50} = 1.1216 \cdot 1.2^{VN}$$

Assuming h_0 equals p_{50} , then, it is possible to establish comparable vulnerability in each system. DIA also indicates that the weapon radius (WR) and lethal radius (LR_{50} —which is a function of p_{50}) relate by

$$WR = \frac{LR_{50}}{1 - \sigma_d^2}$$

²Samuel Glasstone and Philip Dolan (eds.) *The Effects of Nuclear Weapons*. U.S. Department of Defense and U.S. Department of Energy, 1977.

Thus, for a "cookie-cutter" damage function ($\sigma_d = 0$), the weapon radius and lethal radius are equal; for a $\sigma_d = 0.2$, the weapon radius is a bit more than 4 percent larger than the lethal radius.

The difference in SSPK caused by the differing damage sigmas is shown in Fig. B.1. This figure assumes that $LR = LR_{50}$ (i.e., both systems use the same lethal radius). For low values of SSPK, there is very little difference between the two formulations; for fairly high values of SSPK (approaching 90 percent), the differences in SSPK can be a bit over 2 percent.

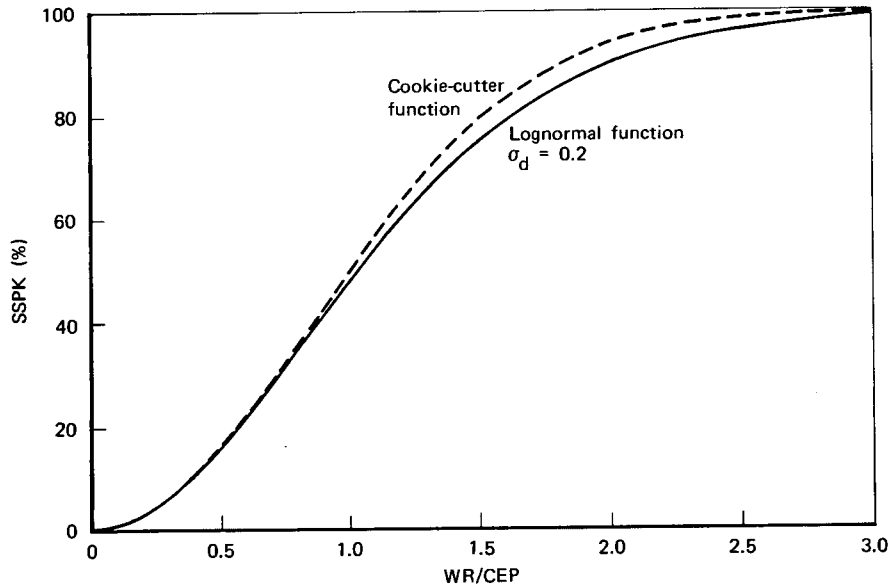


Fig. B.1—Relationship between SSPK and the ratio of weapon radius to CEP for two damage functions

Figures C.1 and C.2 in the next appendix show that the lethal radius of the vulnerability number system is usually equal to or slightly larger than the lethal radius in the traditional model. However, when we compare the weapon radius to the traditional model's lethal radius for ground bursts, the two numbers are roughly equal for tar-

gets of about 2000 psi hardness.³ Thus, for some reason DIA's formulation of weapon radius (for ground bursts) underestimates it by at least 4 percent, based upon their own lethal radius curves. As a result, there is an even greater difference in the SSPK of the two procedures for targets of comparable hardness. This total difference appears to be as much as 4 percent in SSPK.

OVERPRESSURE AND VULNERABILITY NUMBERS⁴

The traditional model of survivability uses a "cookie-cutter" damage function that assumes the target will be destroyed if the overpressure which reaches it is greater than or equal to the target "hardness" (h_o), whereas the target will be undamaged if this overpressure is less than h_o . In the vulnerability number system, though, the overpressure value assigned to a target is the median overpressure (p_{50}) required to kill a target of that type. If a "cookie-cutter" is used with the vulnerability number system ($\sigma_d = 0$), these two hardness values are the same (since, with a "cookie-cutter" function, the median value is also the only value involved). Otherwise, the overpressure rating of the traditional model is not directly comparable to the overpressure in the vulnerability number system. However, as shown above, it is normally assumed that these two overpressures are equal: $p_{50} = h_o$.

In the vulnerability number system, the VN equivalent to a p_{50} overpressure is expressed as

$$VN_o = 12.63 \cdot \text{Log } (p_{50}) - 0.63 .$$

This formula gives the VN directly for 20-kt warheads, which serve as the base for overpressure pulse duration. For larger or smaller weapons, VN_o must be adjusted to determine the true VN base:⁵

$$VN = VN_o - A_{vn}$$

where, for "P" type targets, A_{vn} is derived from

³For example, a VN of 41 (1980 psi) has an LR of 1220 ft, a WR of 1214 ft, and an LR_{50} of 1165 ft for a 1-kt groundburst. At lower target hardnesses, the difference goes as much as 2 percent in the opposite direction, with the $LR_{50} > LR$ for VNs from 5 to 16 (3 to 21 psi). In short, there appears to be a real problem somewhere in DIA's weapon radius formulation.

⁴For more details, see DIA, *Mathematical Background and Programming Aids for the Physical Vulnerability System for Nuclear Weapons*, DI-550-27-4, November 1, 1974.

⁵This is exactly the opposite approach from that used to calculate a weapon radius once the appropriate VN is known.

$$A_{vn} = 5.485 \cdot \ln(W)$$

and where W is found by iteration from

$$W = 1 - \frac{k}{10} + \frac{k}{10} \cdot W^{1/2} \cdot \left(\frac{20}{Y}\right)^{1/3}$$

In this equation, k is the K-factor and Y is the yield in kilotons. For the assumed K-factor of 4 and for the yield equal to 1000 kt, W equals approximately 0.69. This means that A_{vn} equals approximately -2.03 . Since the nominal value of h_o is 2000 psi, by assuming that p_{50} is the same we can calculate that VN_o equals approximately 41.06, so that the VN in the standard representation is about 43.1. Since only integers are used in the vulnerability number system, this becomes 43P4, which is roughly equivalent to a 2000 psi overpressure vulnerability for a 1-Mt warhead.⁶

⁶Alternatively, since VN equals VN_o for a 20-kt warhead, we can say that 41P4 is the rough equivalent of 2000 psi vulnerability for a 20-kt warhead.

Appendix C

COMPLICATIONS IN THE SSPK RELATIONSHIPS

The information presented in Sec. III of R-2577-FF shows the basic relationships between SSPK and its various parameters; however, there are several further uncertainties, problems, and interactions in these formulations, some of which will be described in this appendix. Dealing with these difficulties is an important step in the process of realistically understanding the problems involved in a countersilo strike, as well as in properly assessing the uncertainties of such a strike. The following discussion will focus on the effect of three types of difficulties on the parameter uncertainties and on effective execution of a counterforce attack.

MODELING WARHEAD DESTRUCTIVENESS

There are several texts which attempt to parameterize the overpressure caused at any given distance from the detonation of a nuclear warhead. Figures C.1 and C.2 summarize these data for a 1-kt groundburst and optimum airburst, respectively, with data from *The Effects of Nuclear Weapons* and from DIA's *Physical Vulnerability Handbook*. For groundbursts, the differences are trivial (about 5 percent at most), while for airbursts, the differences are more substantial (up to 18 percent). Comparing the curves in these two figures, it becomes obvious that DIA is more optimistic about the advantages of airbursts against very hard targets.¹ In any case, while these relationships are close to being linear in the log-log frame, their slope does change rather substantially between high and low overpressure values.

¹There is currently some debate over the effectiveness of airbursts at high overpressures because, above about one-half of the traditional "optimum" height of burst, a double-shock waveform develops which tends to reduce the ground range at which a given overpressure actually occurs. However, at about one-half of the traditional "optimum" burst height, airbursts should still significantly increase the range at which overpressure around 2000 psi occurs (by about 9 percent beyond the range for a comparable groundburst). Therefore a compromise between the curves shown in Fig. C.2 is, in reality, probably correct (though based on a lower height of burst). See H. L. Brode and J. G. Lewis, "Implications of Recent Airburst Studies to Damage of Hardened Structures," in W. J. Hall (ed.), *Structural and Geotechnical Mechanics*, Prentice-Hall, Inc., 1975, pp. 55-69; note especially p. 66.

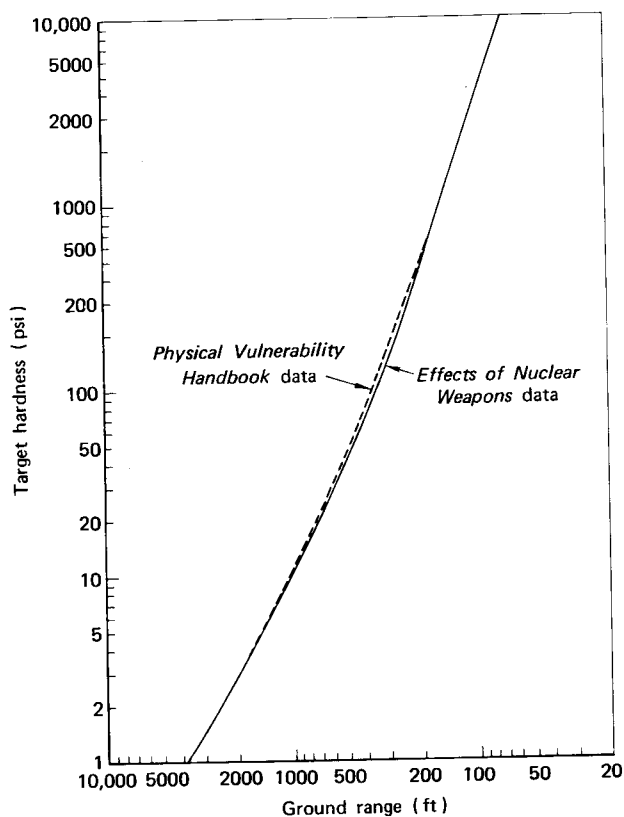


Fig. C.1—Ground range for various overpressure levels for a 1-kt groundburst

The change in slope can be most easily seen by examining the equation for the groundburst curve,² as used in App. B (assuming a 1-kt yield):

$$h = 3.3 \cdot x^{-3} + 6.96 \cdot x^{-3/2}$$

²In Tsipis, p. 20, the following equation is given for the groundburst relationship:

$$h = 3300 \cdot \frac{Y}{x^3} + 192 \cdot \left(\frac{Y}{x^3} \right)^{1/2}$$

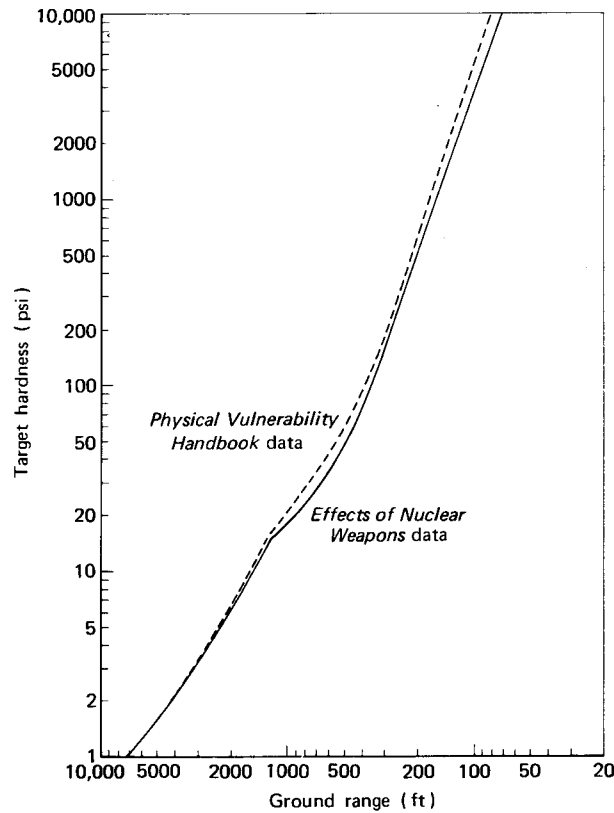


Fig. C.2—Ground range for various overpressure levels for a 1-kt optimal airburst

where Y is the yield in megatons, x is the distance from the detonation in kilofeet, and h is the peak overpressure in pounds per square inch. Using the 1-kt yield of Figs. C.1 and C.2, this becomes

$$h = 3.3 \cdot x^{-3} + 6.07 \cdot x^{-3/2}$$

Tsipis' equation (originally from Brode) produces too low an overpressure at larger ranges (in comparison to *The Effects of Nuclear Weapons* values in Fig. C.1) and should apparently use a number more like 220 instead of 192, or 6.96 instead of 6.07 in the second equation.

In the log-log frame of Fig. C.1 this becomes

$$\text{Ln } (h) = \text{Ln } (3.3 \cdot x^{-3} + 6.96 \cdot x^{-3/2})$$

Taking the derivative to determine the slope:

$$\begin{aligned} d(\text{Ln}h) &= \frac{-9.9 \cdot x^{-4} - 10.44 \cdot x^{-5/2}}{3.3 \cdot x^{-3} + 6.96 \cdot x^{-3/2}} \cdot dx \\ &= \frac{-9.9 - 10.44 \cdot x^{3/2}}{3.3 \cdot x + 6.96 \cdot x^{5/2}} \cdot dx \cdot \frac{d(\text{Ln}x)}{x^{-1} dx} \end{aligned}$$

$$\frac{d(\text{Ln}h)}{d(\text{Ln}x)} = \frac{-9.9 - 10.44 \cdot x^{3/2}}{3.3 + 6.96 \cdot x^{3/2}}$$

Thus, as x becomes small (high overpressures), the slope approaches a value of minus 3; as x becomes large (low overpressures), the slope approaches a value of minus 1.5. Since the x -axis in these figures shows the log of distance decreasing, the negative sign is ignored hereafter.

This change in slope is important because DIA formulates two ways to calculate the SSPK for a target of a specific hardness type (h_o) at a given range (x) from the warhead's actual ground zero.³ The first assumes that SSPK is a function of the distance x :

$$\text{SSPK}_1 = \int_{-\infty}^{z_1} \frac{1}{\sqrt{2\pi}} \cdot e^{-\frac{y^2}{2}} dy$$

$$z_1 = \frac{1}{\beta} \text{Ln} \left(\frac{x_o}{x} \right)$$

$$\beta = \sqrt{-\text{Ln} (1 - \sigma_d^2)}$$

³From DIA, pp. 7-14, 40.

where x_o is the ground range at which overpressure h_o develops. The second formulation assumes that SSPK is a function of the overpressure h that affects the target:

$$SSPK_2 = \int_{-\infty}^{z_2} \frac{1}{\sqrt{2\pi}} \cdot e^{-\frac{y^2}{2}} dy$$

$$z_2 = \frac{1}{\phi} \text{Ln} \left(\frac{h}{h_o} \right)$$

$$\phi = 0.297 \quad (\text{P-type targets})$$

Clearly, $SSPK_1$ must equal $SSPK_2$, which implies that z_1 equals z_2 , or

$$\frac{1}{\beta} \text{Ln} \left(\frac{x_o}{x} \right) = \frac{1}{\phi} \text{Ln} \left(\frac{h}{h_o} \right)$$

Therefore,

$$\text{Ln} (h) - \text{Ln} (h_o) = - \frac{\phi}{\beta} [\text{Ln} (x) - \text{Ln} (x_o)]$$

In other words, the slope (λ) of the lines in Figs. C.1 and C.2 (ignoring the negative sign) equals

$$\lambda = \frac{\phi}{\beta}$$

This formula betrays a problem in DIA's formulations. In their formulations, ϕ and β are each supposed to be constant, while λ is supposed to vary by a factor of 2.⁴ Table C.1⁵ shows how σ_d , which is

⁴This is strictly true in the case where σ_d is capturing only target-to-target variations in hardness. If, however, σ_d includes some warhead-to-warhead variations (e.g., in yield), then this variation needs to be factored out before λ can be the slope of the constant yield lines in Figs. C.1 and C.2. Appendix A discusses these different kinds of variations in more detail.

⁵In this table, the larger values of λ (2.9 and 2.8) correspond to the slope of the curve in Fig. C.1 between about 3000 and 700 psi (λ equals about 2.88 at 2000 psi), while the lower value (1.47) comes from calculating λ based on a σ_d of 0.2 and a ϕ of 0.297.

Table C.1
 σ_d VERSUS ϕ FOR VARYING
 PRESSURE/DISTANCE SLOPES (λ)

$\lambda = 2.9$		$\lambda = 2.8$		$\lambda = 1.47$	
σ_d	ϕ	σ_d	ϕ	σ_d	ϕ
0.1	0.291	0.1	0.281	0.1	0.147
0.102	0.297	0.105	0.297	0.2	0.297
0.2	0.586	0.2	0.566		
0.3	0.891	0.3	0.860	0.3	0.451

a function of β , and ϕ could vary with λ . That is:

$$\lambda = -\phi/\beta$$

Solving for the damage sigma

$$\beta = -\phi/\lambda$$

$$\sqrt{-\ln(1 - \sigma_d^2)} = \beta = -\phi/\lambda$$

$$-\ln(1 - \sigma_d^2) = (\phi/\lambda)^2$$

$$\sigma_d = \sqrt{1 - e^{-(\phi/\lambda)^2}}$$

For the small values of λ ($\lambda = 1.5$) which occur at a few psi overpressure, DIA's assumption that $\sigma_d = 0.2$ and $\phi = 0.297$ for overpressure sensitive targets is probably realistic, and would be expected to be so since ϕ was derived on the basis of "analysis of the Hiroshima-Nagasaki and Nevada test data."⁶ On the other hand, for pressures over 100 or 200 psi, one would expect that relatively little testing of the damage functions has been done since this hardness range became very important only at about the time of the atmospheric test ban. In any case, the different slope ($\lambda = 2.9$ around $h = 2000$ psi) in this range finds a ϕ of 0.297 paired more closely with a σ_d of 0.1, and a σ_d of 0.2 paired to a ϕ of 0.586.

⁶DIA, p. 40. These data are detailed for overpressures of only a few psi.

The effect of the differences in these values of the damage sigma is shown in Fig. C.3 for the nominal target type with p_{50} equal to 2000 psi. For this overpressure λ equals about 2.9. Therefore, using the standard DIA overpressure damage function ($\phi = 0.297$, and thus $\sigma_d = 0.1$) would destroy 99 percent of the targets exposed to 4000 psi, whereas the standard DIA distance damage function ($\sigma_d = 0.2$, and thus $\phi = 0.586$) would destroy only 88 percent of the targets exposed to 4000 psi, and would require about 8000 psi to destroy 99 percent of the targets. Although these variances seem large, Fig. 3 in R-2577-FF indicates that, for the nominal data, a difference of less than 2 percent would exist in SSPK for these differences in σ_d once the CEP and other factors are taken into consideration. Therefore, a σ_d of 0.2 is retained in the text, though it should be clearly recognized that this construct is fairly uncertain (that is, DIA's formulations suggest that σ_d may really equal 0.1 for very hard targets).

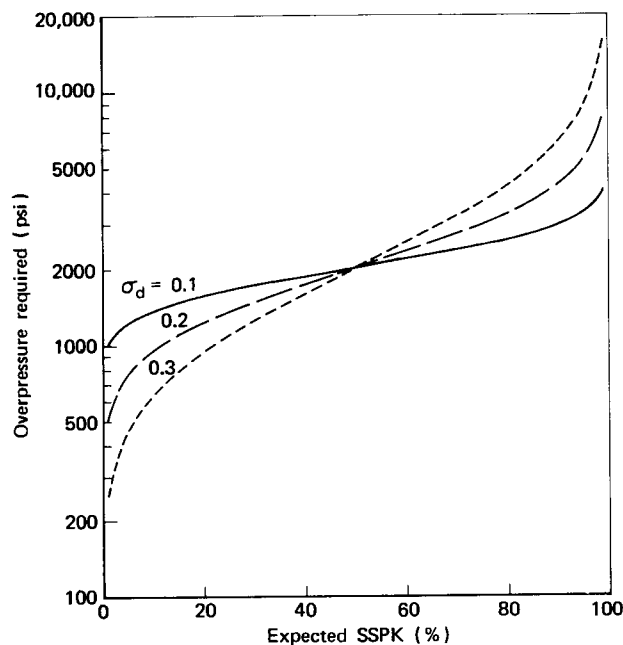


Fig. C.3—Overpressure required for a given SSPK using the DIA damage function

The damage sigma can also be affected by the height of burst chosen. For a weapon targeted at a single target type, a fixed height of burst would probably be chosen that would be optimal for the best estimate of the hardness. This height would then be too high for targets that are harder than expected and too low for those that are softer than expected. The effect of this factor is shown in Fig. C.4. The optimal airburst line is carried over from Fig. C.2, and a second dashed line is added to show the effect if the height of burst is fixed at 100 scaled ft (1000 ft for a 1-Mt warhead). For the harder targets, then, the slope (λ) of the fixed, 100 ft height of burst curve is much lower, suggesting (from Table C.1) that a somewhat higher damage sigma (corresponding to a lower value of the slope λ) would be appropriate for actual airbursts (but not groundbursts) than would otherwise be expected from the data of Fig. C.2. The line running through 2000 psi that corresponds to $\lambda = 1.47$ is added for reference.

There are several other factors that could affect the warhead destructiveness which will not be dealt with in detail here. For example, the data given above assume that the terrain of the target is flat.

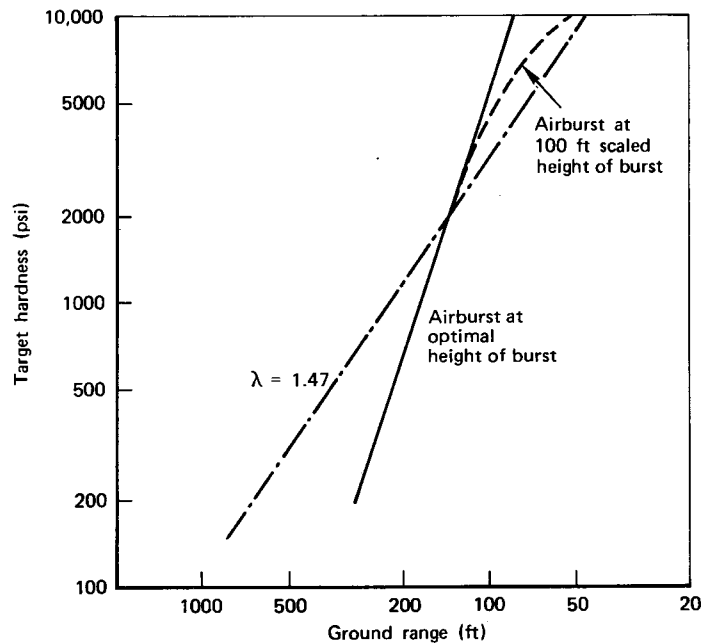


Fig. C.4—Ground range for high overpressure levels for a 1-kt airburst

If, instead, the target is uphill from a detonation, the overpressure felt by the target would be significantly greater at any fixed distance from the ground zero, whereas a downhill slope has the opposite effect.⁷ Similarly, the formulations of the distance/damage relationships could vary with the size, shape, and flexibility of the silo, its orientation to the detonation, and the nature of the soil around the silo.⁸ All of these aspects tend to cause *variations* primarily in silo-to-silo or weapon-to-weapon vulnerability, as opposed to *uncertainty* in the average silo vulnerability. These variations would naturally tend to increase the damage sigma, and thus decrease the nominal SSPK, as shown in Fig. 3 in R-2577-FF.

Finally, in performing the SSPK calculations, it is normally assumed that the weapon radius scales with the one-third power of yield. Although this is a very standard assumption, it may not be perfectly correct.⁹ If this power of yield ($\theta = 0.3333$) is uncertain, then a further uncertainty can be added to SSPK, depending upon the yield at which the testing was done that produced the curves in Figs. C.1 and C.2.¹⁰ For example, a standard deviation of only 5 percent in θ ($\sigma_\theta = 0.01667$) could equate to a standard deviation in a 1-Mt warhead yield of 10 to 30 percent.¹¹ As shown in Fig. 18 in R-2577-FF, that much variance in yield could have a significant effect on SSPK.

ACCURACY COMPLICATIONS

Almost all assessments of ICBM survivability assume that warhead accuracy can be modeled by a circular normal impact distribu-

⁷Glasstone and Dolan, p. 92.

⁸Glasstone and Dolan, pp. 241-242.

⁹Indeed, it is occasionally challenged, as in B. F. Goeller and R. D. Specht, *Some Implications of Uncertainties in the Hiroshima Explosion*, The Rand Corporation, RM-4725-TAB, November 1966, pp. 5-9.

¹⁰That is, if the curves in Figs. C.1 and C.2 are based on 1-Mt test shots assuming $\theta = 0.3333$, then any other value of θ would only affect weapon radius calculations at yields other than 1 Mt. Further, the greater the difference in the yield used in the tests and the actual yield used in a countersilo strike, the greater the effect different values of θ can have.

¹¹These uncertainties assume that U.S. knowledge of the data in Figs. C.1 and C.2 comes largely from small-yield tests (1 kt to 100 kt) at the Nevada Test ground, as opposed to the larger megaton range tests at the less well instrumented Pacific Island test sites.

tion. There are two ways in which this assumption could fail to hold. First, the distribution of impacts may not be circular. Second, the impacts may not be normally distributed. Both of these problems can affect the SSPK estimates, although in reality their actual effect may be somewhat difficult to ascertain.

The design of missile guidance systems makes it likely that the distribution of warhead impacts may not be circular. Normally, certain aspects of guidance error lead to a downrange error, whereas other aspects lead to a crossrange error. Therefore, in calculating the CEP from test data, a mean point of impact and standard deviation is usually calculated separately for the downrange and crossrange directions. Only if both standard deviations are approximately equal can the distribution be assumed to be circular.¹²

The importance of the circularity assumption is demonstrated in Fig. C.5. Here, the true SSPK is compared to the calculated SSPK for varying ratios of the downrange error (σ_D) to the crossrange error (σ_C).¹³ The difficulty in this procedure is trying to find a simple mathematical formulation for CEP from σ_D and σ_C . If, as is normally done, CEP is assumed to be proportional to the sum of these two error terms,¹⁴ then there is a good fit between the actual SSPK and that calculated using this approximate CEP if it equals 1200 ft and the ratio of σ_D/σ_C is between 0.25 and 4. On the other hand, this same CEP approximation is relatively poor for a 600-ft "approximate CEP" if σ_D and σ_C are not close to being equal. In this later CEP range, the root

¹²For the impact distribution to be truly circular, both standard deviations must be equal, and the crossrange and downrange error cannot be correlated. Note that, given a standard reentry angle of less than 30 deg, the downrange impact error is a projection of the downrange error along the line of flight, multiplying the line of flight error by at least a factor of 2. Therefore, for circular impact errors, the downrange error along the line of flight must be much less than the corresponding crossrange error.

¹³In Fig. C.5, the actual SSPK is calculated on the basis of 2000 simulations for the given σ_D/σ_C ratio, whereas the $\sigma_C + \sigma_D$ and the $\sqrt{\sigma_D^2 + \sigma_C^2}$ approximations of CEP are calculated and used in the normal SSPK damage formula. A systematic bias of zero is used to simplify the calculations.

¹⁴Or, in a strict mathematical sense, since $CEP = 1.1774 \cdot \sigma$, then

$$\begin{aligned} CEP &= 1.1774 \cdot \left(\frac{\sigma_D + \sigma_C}{2} \right) \\ &= .5887 \cdot (\sigma_D + \sigma_C) \end{aligned}$$

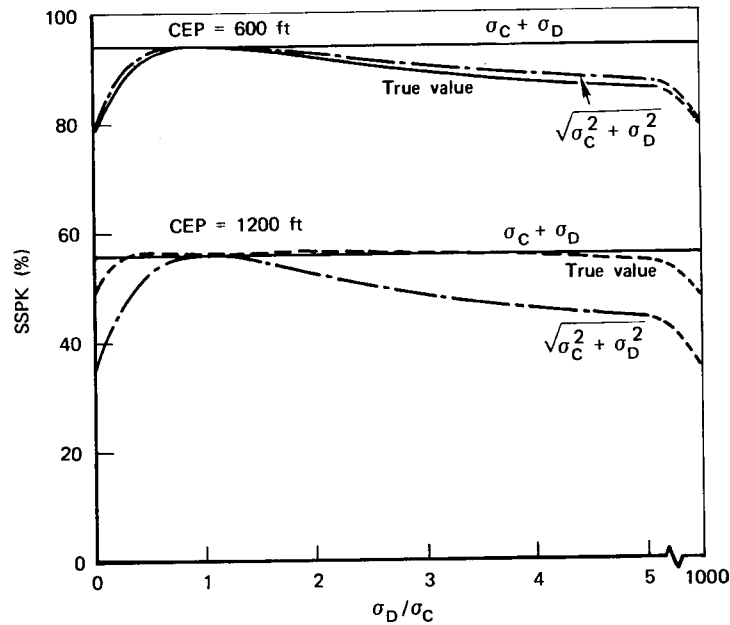


Fig. C.5—Comparison of true SSPK to SSPK based on CEP approximations

mean square¹⁵ of σ_D and σ_C is a better approximation, but it is not a good approximation for a CEP of 1200 ft. In other words, neither of these simple procedures for deriving CEP from σ_D and σ_C works universally well unless σ_C and σ_D are approximately equal. If σ_D and σ_C are much different, then a fairly large error can occur in the SSPK calculation depending upon the way in which CEP is calculated¹⁶ and the magnitude of that CEP in comparison to the weapon radius. Specifically, the normal procedure of averaging σ_C and σ_D tends to overestimate SSPK if the SSPK value is high.

The second problem with warhead accuracy is a result of the

¹⁵In a strict mathematical sense,

$$\begin{aligned} \text{CEP} &= 1.1774 \cdot \sqrt{\frac{\sigma_D^2 + \sigma_C^2}{2}} \\ &= 0.8325 \cdot \sqrt{\sigma_D^2 + \sigma_C^2} \end{aligned}$$

¹⁶A geometric mean of σ_C and σ_D was also tried, and its results were even worse.

nature of the impact distribution. The actual shape of the distribution in either downrange or crossrange directions may not be a normal distribution. However, it is very difficult to ascertain what the true distribution should be (or to prove that the distribution is not normal), especially on the basis of a relatively small number of flight tests. For example, a normal impact distribution for a 600-ft CEP is shown as the solid line in Fig. C.6. An alternative, 800-ft CEP distribution that

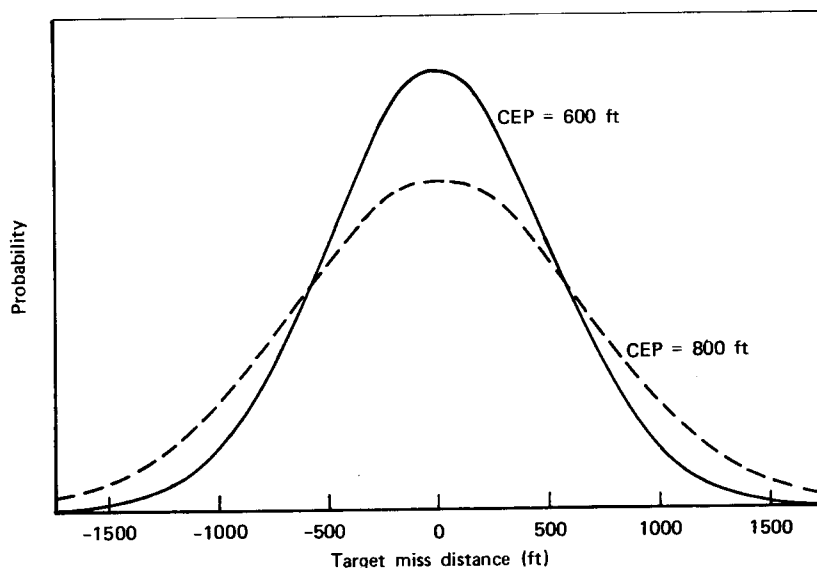


Fig. C.6—Alternative distributions for downrange or crossrange miss distance

places greater emphasis on the tails of the distribution (and which is also normal, though it need not be¹⁷) is shown as the dashed line in this figure. Although these distributions lead to significantly different SSPKs (93 percent versus 81 percent, as shown in Fig. 7 of the text), it could take up to 95 flight tests to determine which distribution is correct (to the 97.5 percent, one-tailed confidence level),¹⁸ even if these

¹⁷As indicated on Fig. C.6, the dashed line distribution has a CEP one-third greater than the solid line distribution. This somewhat more spread distribution is specified as a normal distribution to make comparison of both distributions statistically easier.

¹⁸The difference between these two normal distributions is measured effectively by the difference in their CEPs, which can be tested with a χ^2 test. For a large number of

are the only two distributions considered as real possibilities. Naturally, just for normal distributions, a whole continuum of "real possibilities" exists, and when other possible distributions are added, determining the true distribution for weapon accuracy is impossible.

Impact distributions other than the normal can distort the SSPK significantly, in turn raising again the question of how CEP should be calculated. In Fig. C.7, we compare the cross-sections of a circular Student's t distribution with two degrees of freedom to a circular

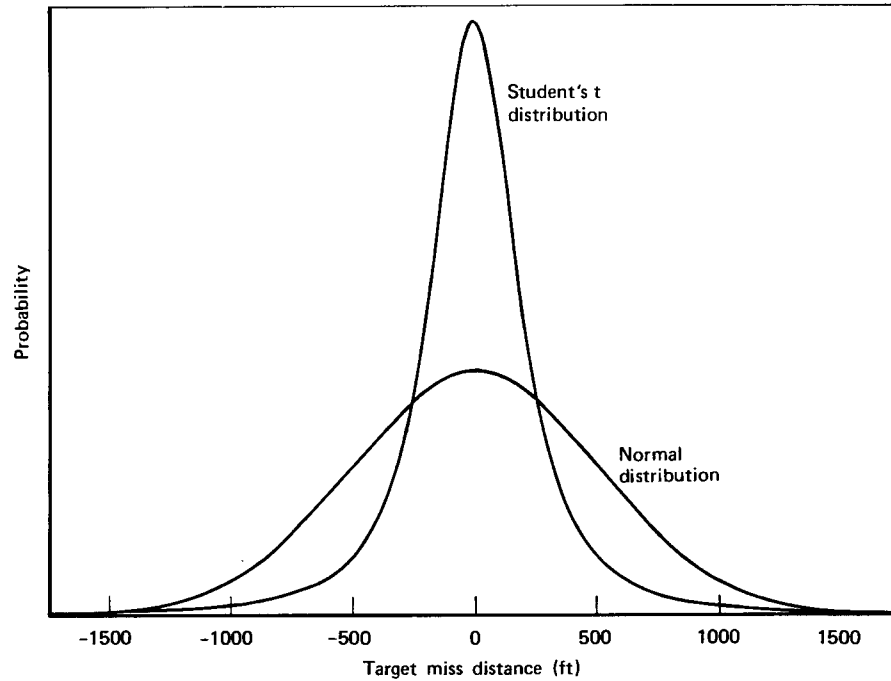


Fig. C.7—Comparison of two impact distributions with equal CEPs calculated from standard deviations

tests ($T \geq 31$), an observed CEP can be definitely determined to be attributable to one of two (and only two) possible true CEPs (CEP_1 and CEP_2) with probability $1 - \alpha$ if

$$\frac{1 - \alpha \chi^2_{T-1}}{2} \leq \left(\frac{CEP_2}{CEP_1} \right)^2$$

where $CEP_2 \geq CEP_1$. For this example, the CEP ratio is 4/3, $1 - \alpha = .975$, ${}_{.975}\chi^2_{94} = 122.718$, and ${}_{.025}\chi^2_{94} = 69.062$, so that $1.7769 \leq 1.7777$ for $T = 95$.

normal distribution, both distributions having a 600-ft CEP calculated by summing the downrange and crossrange standard deviations. Assuming zero systematic bias, when combined with the nominal attack data these two distributions yield SSPKs of 96 and 94 percent, respectively, a fairly significant difference, especially if viewed from the perspective of the SSPS. However, by the standard definition, CEP is supposed to be the distance within which half of the impact points fall; by this definition, this Student's *t* distribution has a 280-ft CEP, and thus theoretically a 100 percent SSPK (compared to the estimated 96 percent SSPK). Further, if the Student's *t* is broadened to produce a 600-ft CEP according to the standard definition, the true SSPK falls to about 83 percent. In short, the standard definition of CEP—the distance within which half the impact points fall—is a poor way to derive the CEP, since analysts can never be really certain whether the impact distribution is circular normal. Rather, the standard calculation technique, using the sum of σ_C , and σ_D , is a much better way to derive the value for CEP.

HEIGHT OF BURST UNCERTAINTY AND ACCURACY

Uncertainty in the actual height of an airburst has two kinds of effects on warhead accuracy.¹⁹ First, a systematic error in the height of burst causes a proportional (though larger) systematic impact bias to be added to the downrange component of accuracy. This is illustrated in Fig. C.8, where the warhead is intended to detonate at point A, at height of burst HOB_o , directly over the target (assuming perfect accuracy). If, instead, every warhead's fuze mistakenly detonates at height of burst HOB' causing the warhead to travel too far (or too short) in the downrange direction, an extra "HOB-caused bias" is added to the normal systematic bias. For reentry angles (β_r) of 22 to 27 deg, this HOB-caused bias will be about 2 to 2.5 times the systematic error in height of burst ($HOB_o - HOB'$).²⁰ The effect of this

¹⁹Airbursts generally affect (negatively) both the accuracy and reliability of a warhead, as indicated in *Analyses of Effects of Limited Nuclear Warfare*, Subcommittee on Arms Control, International Organization and Security Agreements of the Committee on Foreign Relations, U.S. Senate, September 1975, pp. 7-8. Only the effect of airbursts on accuracy will be considered here.

²⁰Geometrically, this bias (B_h) is simply $B_h = (HOB_o - HOB') \cdot \cot \beta_r$, where $\cot (22^\circ)$ is 2.48 and $\cot (27^\circ)$ is 1.96. The value of 22 deg will be used here since it is cited as realistic in John Steinbruner and Thomas Garwin, "Strategic Vulnerability: The

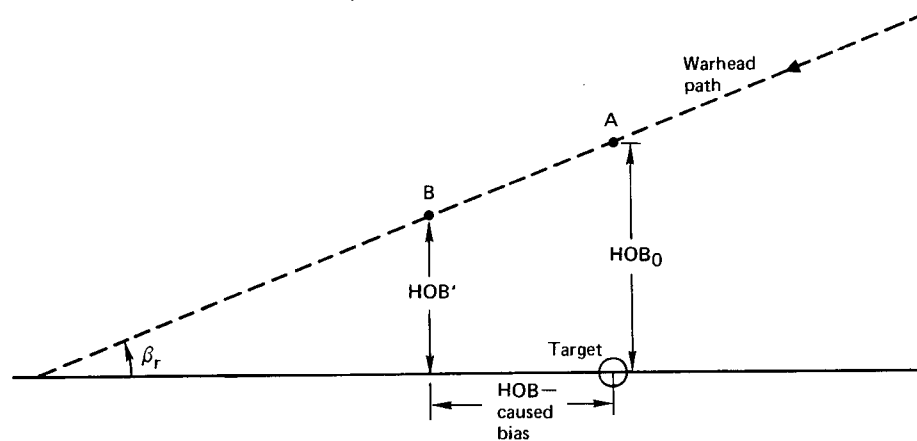


Fig. C.8—Airburst schematic diagram

accuracy error is, naturally, difficult to predict since the systematic bias of the guidance system will not necessarily be in the same direction (indeed, it could be in the opposite direction and therefore cancel out). For the nominal example (with a basic systematic bias of 200 ft), the net bias will be in the range of $200 \pm B_h$ ft, or 0 to 450 ft if the systematic error in height of burst is 100 ft. The relative impact of this error can be read directly from Fig. 8 in R-2577-FF.

The other kind of error in height of burst is the random error, due to variations in the fuzing mechanism between warheads or to differing conditions around each target (such as an error in measuring the

Balance Between Prudence and Paranoia," *International Security*, Summer 1976, p. 175; a value of 22 to 24 deg is also given in Clarence Robinson, "U.S. Weighs New SALT Offer to Soviets," *Aviation Week and Space Technology*, September 4, 1978, p. 24. Note that it will be assumed here that the terrain in which the warhead impacts is level, thus making the reentry angle β_r the angle between the reentry path and the ground.

There are, of course, different mechanisms for determining the burst point of an airburst. For most of these mechanisms, called fuzes, the reentry angle is the critical parameter determining the height of burst uncertainty effect on accuracy. However, radar fuzes measure the actual height above the ground, perhaps the most accurate form of fuzing. Unfortunately, variations in terrain slope will cause changes in the reentry angle between targets, increasing any silo-to-silo impact variations due to errors in the height of burst for radar fuzes. Thus, the results that are shown here may really be somewhat conservative.

exact altitude of the target).²¹ This kind of error causes some warheads to detonate too high and others too low, affecting accuracy by adding to the downrange inaccuracy. In order to parameterize this effect on accuracy, it will be assumed that the random height of burst error is normally distributed around the systematic height of burst error (which could be zero), having a standard deviation of σ_h . The effect of this extra error on the CEP is illustrated in Figs. C.9 and C.10.²² As is clearly indicated, lower reentry angles increase the magnitude of the new CEP (CEP'); the new CEP is also larger if the crossrange error was

²¹This kind of difficulty is discussed in *Counterforce Issues for the U.S. Strategic Nuclear Forces*, The Congress of the United States, Congressional Budget Office, January 1978, p. 12. Note especially footnote 5. Data on pp. 64 and 70 of that report under Assumption 4 are close to the values shown in Fig. C.10 below.

²²If the downrange impact distribution is initially distributed as $N(O, \sigma_D^2)$, the random height of burst error changes this distribution to $N(O, \sigma_D^2) + N(O, \sigma_h^2 \cot^2 \beta_r)$, or $N(O, \sigma_D^2 + \sigma_h^2 \cot^2 \beta_r)$. Thus, if CEP was

$$\text{CEP} = 0.589 (\sigma_C + \sigma_D)$$

then the new CEP (CEP') can be expressed as

$$\text{CEP}' = 0.589 \cdot \left(\sigma_C + \sqrt{\sigma_D^2 + \sigma_h^2 \cdot \cot^2 \beta_r} \right)$$

Thus the ratio of final to initial CEP is

$$\begin{aligned} \frac{\text{CEP}'}{\text{CEP}} &= \frac{0.589 \cdot \sigma_C + \sqrt{\sigma_D^2 + \sigma_h^2 \cdot \cot^2 \beta_r}}{0.589(\sigma_C + \sigma_D)} \\ &= \frac{\sigma_C}{\sigma_C + \sigma_D} + \sqrt{\frac{\sigma_D^2}{(\sigma_C + \sigma_D)^2} + \left(\frac{0.589 \cdot \sigma_h \cdot \cot \beta_r}{\text{CEP}} \right)^2} \end{aligned}$$

For $\sigma_C = \sigma_D$, this simplifies to

$$\frac{\text{CEP}'}{\text{CEP}} = 1/2 + \sqrt{1/4 + (0.589 \cdot \cot \beta_r) \cdot \left(\frac{\sigma_h}{\text{CEP}} \right)^2}$$

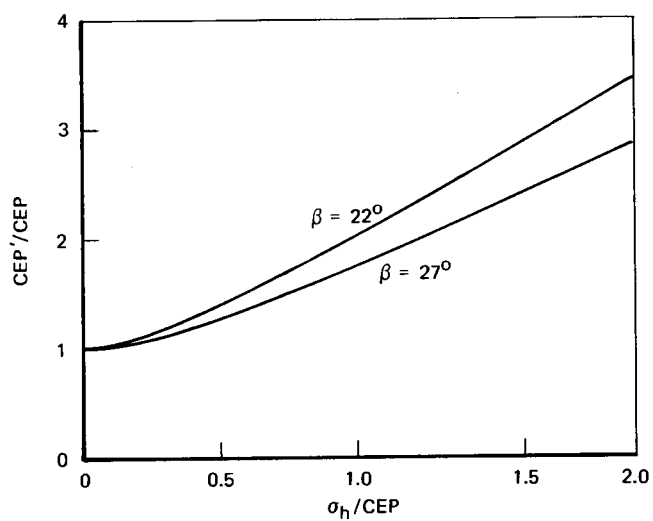


Fig. C.9—Effect of random uncertainty in HOB on CEP for differing reentry angles, $\sigma_D = \sigma_C$

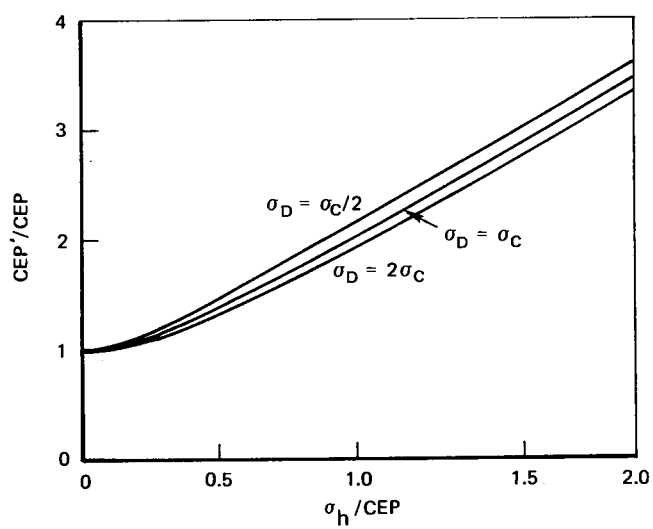


Fig. C.10—Effect of random uncertainty in HOB on CEP for differing ratios of $\sigma_D : \sigma_C$, $\beta = 22^\circ$

initially greater than the downrange error. In any case, if the error in the height of burst is much greater than about one-fourth of the original CEP (σ_h/CEP is greater than 0.25), the effect on the actual CEP of the error in height of burst can be significant.²³

Ideally, airbursts are preferred to groundbursts because they lead to a higher SSPK (compare the lethal radii in Figs. C.1 and C.2) and lower collateral damage from fallout. However, the above uncertainties in the height of burst will degrade the SSPK of an airburst, while generally not affecting the SSPK of a groundburst. To maximize SSPK, it is important to know the magnitude of uncertainty in height of burst that would lead to a preference for groundbursts (though errors in target altitude estimates could still cause some "height of burst" type errors even with groundbursts). As can be seen in Fig. 1 of R-2577-FF, the nominal SSPK is about 93 percent for an optimal airburst, or 89 percent for a groundburst. Therefore, a groundburst with an SSPK of 89 percent would be preferred (on the basis of effectiveness) if the SSPK of the airburst dropped below 89 percent because of height of burst uncertainty.

Figure 8 in R-2577-FF indicates that a total systematic bias of about 430 ft (instead of the nominal 200 ft) would lower SSPK to 89 percent for the airburst. For a reentry angle of 22 deg, a systematic height of burst error of 254 ft or more would guarantee at least this level of systematic bias, and a systematic height of burst error less than 93 ft would leave the airburst preferred (assuming no other uncertainty).²⁴ Systematic errors in height of burst between these two values could also be sufficient to make groundbursts preferred, depending upon the relative direction of the nominal systematic bias and the height of burst error. Naturally, if the initial systematic bias were larger (or smaller) than 200 ft, this range would be relatively larger (smaller). Further, this estimate ignores the effect that a systematic error in height of burst would have on the weapon radius itself. Thus, according to Fig. 5 in R-2577-FF, a 250-ft error in height of burst would, by its effect on the weapon radius, lower the SSPK from 93 percent to about 92.5 percent on the low side and 91.5 percent on the high side; for these lower values of the weapon radius, even less

²³This ignores (and tends thus to underestimate) the added effect of a downrange error that will now be larger (in most cases) than the crossrange error, as discussed above.

²⁴That is, even if the height of burst error is in the opposite direction of the original 200-ft error, it need only be 630 ft to produce the desired net effect (which would result from a 254-ft error in burst height ($630/2.48$)). Alternatively, if the two errors are in the same direction, the minimum required height of burst bias is 230 ft, or a 93-ft error in burst height ($230/2.48$).

systematic bias than the 93- to 254-ft range would be required to lower the net SSPK below 89 percent.

The effect of the random height of burst error can be calculated somewhat more generally. Where the systematic bias is relatively small, the major determinant of SSPK is the ratio of the weapon radius to the CEP. Moving from a groundburst to an optimal airburst increases the weapon radius, and will also increase the CEP by adding the effect of random height of burst error. As a first approximation, an airburst will be preferred if the increase in weapon radius is greater than the increase in CEP. The regions where this is true are shown in Fig. C.11 for wide range of effective target hardnesses.²⁵ For the range of interest (VNs above about 37), the standard deviation of the random height of burst error (σ_h) must be less than 20 to 30 percent of the CEP for an airburst to be preferred. For a 600-ft CEP, this implies a σ_h of less than 120 to 180 ft. For much greater accuracies (as are being discussed for the MX and other future systems), the

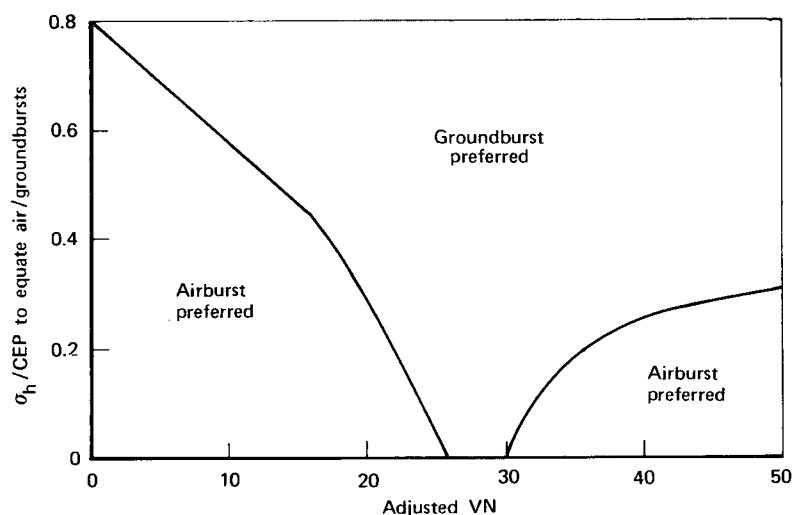


Fig. C.11—Effect of height of burst uncertainty on preference for airbursting

²⁵The adjusted VN is the initial VN adjusted for the K-factor. Therefore, in our example, the adjusted VN (VN_0) is about 41. The adjusted VNs should equate to standard overpressure values. See App. B.

range of critical values for σ_h is correspondingly lower. Naturally, σ_h values even of this magnitude will also lower somewhat the average SSPK by lowering the weapon radius at the extreme values of the actual height of burst. This point is illustrated in Fig. C.12 for an adjusted VN of 42, where a σ_h of 120 to 180 ft lowers the average SSPK by 0.5 to 1.0 percent. Figure C.12 also shows that if the σ_h were as large as 300 ft, groundbursts would be preferred to airbursts simply because of the effect of variability in burst height on the weapon radius, ignoring its impact on CEP. This latter point is true for all adjusted VNs from 38 to 50, given an initial CEP of 600 ft.²⁶

In short, it does not take much of an error in airburst fuzing to make groundbursts preferred to airbursts on the grounds of effectiveness. A 200-ft error in either the average height of burst or in the random variation around that average is sufficient, alone, to make

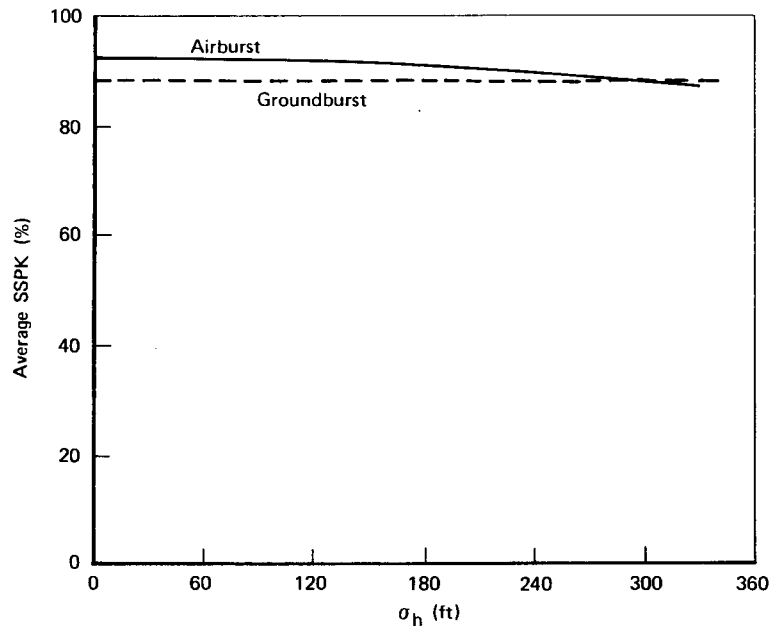


Fig. C.12—Degradation of average SSPK due to effect of height of burst uncertainty on weapon radius

²⁶Higher values of CEP allow for larger values of σ_h before groundbursts are preferred.

airbursts relatively less effective. Indeed, for the example given, these errors must be held to less than 100 ft, and perhaps less than 50 ft (when both effects are combined), to guarantee that airbursts will be preferred.²⁷

²⁷At least one source suggests that the extent of this error is about 320 ft (20 percent of the claimed optimal 1600 height of burst). See *Counterforce Issues for the U.S. Strategic Nuclear Forces*, pp. 64, 70.

Appendix D

DERIVATION OF THE FORMULA FOR THE IMPACT DISTRIBUTION OF THE "CLOSEST" WARHEAD

Let $(x_1, y_1), \dots, (x_n, y_n)$ be the points of impact for the n warheads assigned to a target. It is assumed that these points are independent and have circular normal distributions such that for all i :

$$E(x_i) = E(y_i) = 0$$

$$\text{VAR}(x_i) = \text{VAR}(y_i) = \sigma^2$$

Then, for any pair (x, y) , consider their distance R_i from the target, and define U such that:

$$R_i = \sqrt{x_i^2 + y_i^2}$$
$$U = R^2/\sigma^2 = \left(\frac{x}{\sigma}\right)^2 + \left(\frac{y}{\sigma}\right)^2$$

Since U is the sum of squares of two independent standard normal variates, U has a chi-square distribution with two degrees of freedom (χ^2_2), or negative exponential, the cumulative distribution function being expressed as

$$F(u) = \begin{cases} 1 - e^{-U/2} & \text{for } u > 0 \\ 0 & \text{for } u \leq 0 \end{cases}$$

Now, in general, let $u_i = R_i^2/\sigma^2$; thus the distance to the closest impact equals $\min(u_i)$. Then the cumulative distribution function for the closest impact point can be derived as

¹I am indebted to Gus Haggstrom of Rand for providing this derivation. The use of variables U and R in this appendix does not conform to their standard use in the rest of the report and in the Glossary.

$$\begin{aligned}
G_1(u) &= P[\min(u_i) \leq u] = 1 - P[\min(u_i) > u] \\
&= 1 - \prod_{i=1}^n P(u_i > u) = 1 - [1 - F(u)]^n \\
&= 1 - e^{-nu/2}
\end{aligned}$$

or, for the closest distance in unnormalized (R) terms

$$G_1(R) = 1 - e^{-\frac{n}{2} \cdot \left(\frac{R}{\sigma}\right)^2}$$

This is in contrast to the standard cumulative distribution function of a warhead's impact:

$$F(R) = 1 - e^{-\frac{1}{2} \cdot \left(\frac{R}{\sigma}\right)^2}$$

To make a direct comparison, the cumulative distribution function of the closest impact point can be changed to

$$G_1(R) = 1 - e^{-\frac{1}{2} \cdot \left(\frac{R}{\sigma/\sqrt{n}}\right)^2}$$

Thus, the closest point has a standard deviation (and therefore a CEP) which is smaller than the overall standard deviation (or CEP) by a factor of one over the square root of the number of warhead impacts.

Note that this formulation assumes a systematic bias of zero and a perfect circular normal impact distribution.

Appendix E

PHYSICALLY MODELING FRATRICIDE

In Sec. IV of R-2577-FF, two models are presented of the impact of fratricide on incoming warheads. The first is based on an article by Steinbruner and Garwin in *International Security*. The results of that article are reported to come from a physical model of fratricide, in which warheads are destroyed by flying through the stems or clouds of primarily uprange nuclear detonations. Steinbruner and Garwin's physical description of the fratricide problem offers an excellent point of departure for discussing this physical phenomenon and models of it.

THE PHYSICS OF FRATRICIDE

According to Steinbruner and Garwin, there are two periods after the detonation of a nuclear warhead when its effects can be deadly to other incoming warheads. The first period begins at the detonation itself and ends "following the initial radiation pulse from a nuclear explosion."¹ The second period begins at the propagation of the cloud stem, "no more than 10 seconds later . . . ," and ends many minutes later when debris particles of a lethal size (nominally assumed by the authors to be 10 grams) have fallen back to the earth out of the cloud and stem.² For a 1-Mt warhead, this time is assumed to be at least five minutes. Thus, the two periods when a second warhead could be delivered to a target and avoid fratricide are from a couple to ten seconds after the first warhead explodes, and after several minutes. Steinbruner and Garwin argue against the use of the first "window" because they do not feel that such a rigid time interval could be adhered to.³ Therefore, to avoid local fratricide, they use the second

¹Steinbruner and Garwin, p. 151, footnote 14.

²Steinbruner and Garwin, p. 151, footnote 14; pp. 178-181.

³Their argument is that "human factors" will lead to most of a one minute average timing error, since fully automated launch is unlikely. At very least, this ignores a long military tradition of "synchronizing watches" (or clocks) and executing military plans at a fixed time rather than as soon after the order is given as is possible. Since overcoming fratricide is clearly in the Soviets' favor, it only seems logical that they would indeed use some such measures.

window and require that warheads have at least six minutes between timed arrivals at the same target.

Steinbruner and Garwin clearly ignore one of the easiest ways to use the first window: delivery of a second or third warhead from the same booster. Such a procedure removes variations of launch time, and separates the warheads only by the difference in flight time along a flight path after separation and by variations (slight errors) in this flight time. At least theoretically, the flight paths can be chosen to produce any separation in arrival time that is desired; thus variations should be the only problem in using the first window. Such variations cannot be very great, for the earth is turning as the missile is in flight, and a delay of even one second in the actual flight time would place the target 1000 to 1200 ft east of its planned location, depending upon how far north the targeted missile field is. Thus, for a 600-ft CEP, it is reasonable to assume that variations in flight time cannot be more than a few tenths of a second. The primary difficulty of using two or more warheads from the same booster is that an unreliable booster will allow the survival of each target it is to cover.⁴

If, instead, warheads are used from different boosters, two additional sources of error can enter the timing. One is the timing with which the missiles are "executed" (the button is pushed), relative to each other, and the other is variation in the time between execution and actual launch of the booster (as flight time, for guidance purposes, must begin with the actual lift-off of the missile). The relative time of booster execution should be easily controllable by using synchronized clocks and execution times, at worst, or missiles from the same squadron under control of the same launch control center, at best. These errors should then be very small. And while this author knows little of the execution-to-lift-off sequence of events, especially for Soviet missiles, he does know that Minuteman missiles require about 30 to 50 seconds for this sequence,⁵ which would imply that errors should again not be too great; a standard deviation measured in seconds would probably capture such errors.

The development of the cloud rise dynamics in the DELFIC fallout model gives us perhaps the best way for approximating the actual length of the first window. In the DELFIC model, the cloud development proceeds through four phases, the first three of which are of interest here: (1) the fireball phase, (2) the fireball transition phase,

⁴This is the problem of dependent reliabilities, as mentioned in R-2577-FF. Using warheads from the same booster also causes booster accuracy errors to be transmitted to every warhead thereon, causing a correlation of miss distance (a bias on a missile-to-missile variation basis). See App. A.

⁵*Ballistic Missile Staff Course Study Guide*, 4315 Combat Crew Training Squadron, Vandenberg Air Force Base, May 1, 1978, pp. 2-10.

and (3) the entrainment rise phase.⁶ The fireball phase begins with warhead detonation and continues through the growth of the fireball. This phase includes most of the prompt effects that would be lethal to a second incoming warhead (both blast and radiation), and thus once it is completed, the window should begin. The second phase involves only a slight expansion of the fireball, accompanied by the development of a strong vortex circulation within the fireball that will eventually lead to its fast rise and rapid entrainment of potentially lethal, small solid debris particles. However, at this stage, for a 1-Mt weapon, most of the entrainment is of ambient air, and the solid particles that have been entrained are largely vaporized. Therefore, a second warhead entering the same area during this phase would probably survive. In phase 3, the cloud begins to rapidly rise, cooling the fireball; solid (nonvaporized) particles are entrained (taken up) into the cloud; and the previously vaporized particles begin to solidify as the cloud cools below their vaporization point. Thus, by phase 3, the destructive particles Steinbruner and Garwin focus on are in the cloud, and would probably cause the fratricide of other incoming warheads.

According to the DELFIC manual, phase 3 begins roughly 6.5 to 8 seconds after detonation for a warhead of about 1-Mt yield, depending upon the exact yield and the height of burst. Phase 2 is supposed to begin just before the second fireball temperature maximum, roughly 0.9 to 1.1 seconds after detonation for a 1-Mt warhead.⁷ However, *The Effects of Nuclear Weapons* shows that radiation effects are significant for perhaps two to three seconds after detonation,⁸ suggesting that the real window is from two or three seconds out to about 6.5 to 8 seconds (and within Steinbruner and Garwin's 10-second maximum).

A SAMPLE CALCULATION OF FRATRICIDE IN THE EARLY WINDOW

To show the potential impact of fratricide in the early window, it will be assumed that the window itself lasts from 2.5 to 7.5 seconds

⁶The latter two names are mine, with which I try to describe more clearly the physical phenomena important to fratricide. See H. G. Norment, W. Y. G. Ing, and J. Zuckerman, *Department of Defense Land Fallout Prediction System, Volume II—Initial Conditions*, Technical Operations Research, DASA-1800-2, September 1966, pp. 3-8. DELFIC is probably the most detailed model available for description of what physically occurs in the production of fallout.

⁷Norment et al., pp. 7-8.

⁸Glasstone and Dolan, pp. 311, 530.

after the detonation of a warhead. It will also be assumed that the error in arrival time is an independent, normal variable for each warhead with a standard deviation σ_t ; further, all warheads are assumed to arrive on target (reliability equals 100 percent).

For a two-warhead attack, it is clearly optimal to time the second warhead five seconds behind the first, in the middle of the assumed window. Based on this assumption, Fig. E.1 shows the probability that the second warhead survives fratricide, given a normal distribution for the timing error as assumed above for each warhead. Under these assumptions, a σ_t of 2.6 seconds would roughly correspond to a 50-percent fratricide survival probability (the dashed line) of the second warhead, the level given in the local fratricide model shown in Fig. 33 in R-2577-FF. For longer times, the probability of the second warhead surviving fratricide declines quickly, much as Steinbruner and Garwin argue in their article.

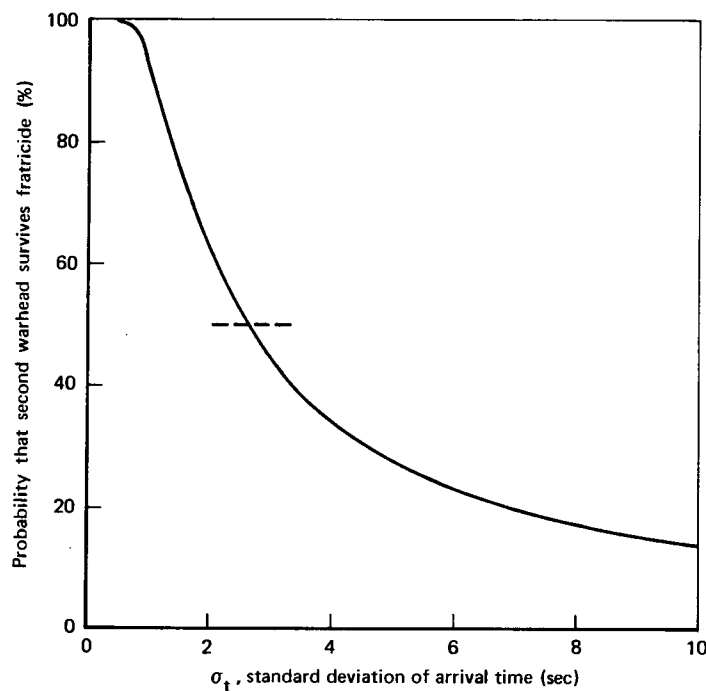


Fig. E.1—Effect of fratricide on a warhead timed to arrive in the first window after a previous nuclear detonation on the same target

Figure E.2 shows the cumulative probability that two or three warheads would survive local fratricide in a four-warhead attack.⁹ Here, the warheads are timed at 0, 2.5, 5.0, and 7.5 seconds,¹⁰ so that a zero standard deviation would allow all four warheads to detonate (each falling barely within the windows of the others), whereas even the slightest error in timing would make it impossible to have more than three survive fratricide (thus, if the second warhead is a little late, it will either kill the third warhead in its first 2.5 seconds, or the fourth warhead will be killed by either the third or the first warhead). In any case, using the data from Fig. 33, the local fratricide model

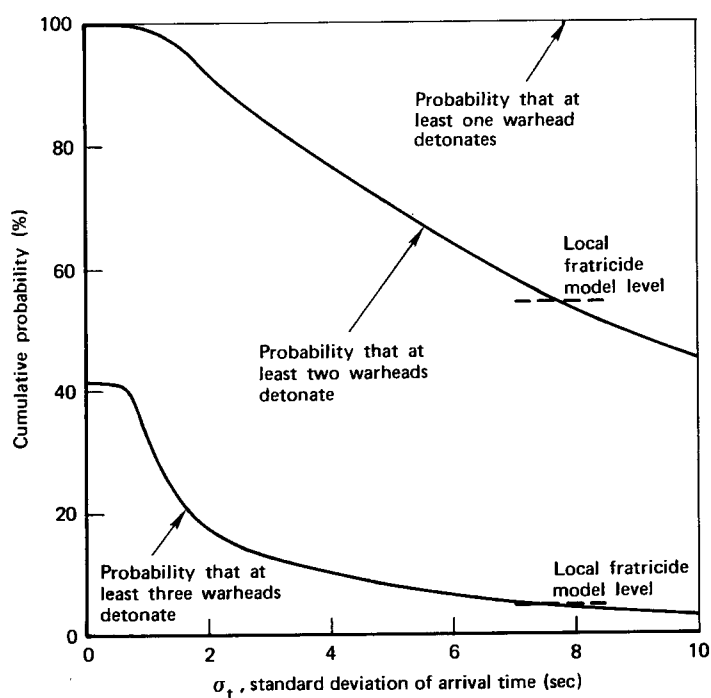


Fig. E.2—Probability that warheads will survive fratricide and detonate if four warheads are assigned to a target with various delays

⁹These results are based upon 4000 Monte Carlo simulations of the actual timing.

¹⁰Other delays might be optimal for large timing errors, although this possibility was not examined.

would predict that at least three warheads would detonate about 5 percent of the time, and at least two warheads would detonate about 54 percent of the time (the two dashed lines in Fig. E.2). In each case, the corresponding σ_t is from seven to eight seconds, a much larger timing error than that allowed by two warheads as indicated in Fig. E.1.

This result shows that the local fratricide model used in text is too simple because it ignores the fact, shown in Figs. E.1 and E.2, that the use of more warheads at staggered intervals improves the probability that a second warhead will detonate for the same level of timing error. A model that reflects this phenomenon would thus be preferable to the simple local fratricide model used in the text. On the other hand, the relatively nice "fit" of the local fratricide model data to the physical model (for a 7 to 8 second timing error) shown in Fig. E.2 indicates that there is at least some basis for thinking that the local fratricide model may be a reasonable estimate of local fratricide. And while the uncertainty in the window timing or quality¹¹ is not captured in Fig. E.2, it can be argued that these uncertainties would contribute to the variance in the fratricide estimates shown in Fig. 35 in R-2577-FF (along with uncertainty in the timing error).

PROBLEMS WITH THE SECOND WINDOW

The important parameters of the second window are the time at which it opens and the size of the cloud until it does. Steinbruner and Garwin's analysis is somewhat confused, especially concerning the second point. Initially, they give the cloud stem radius as 1 (although they indicate no units, miles are implied), and a cloud radius 2.2 times the stem radius for a 1-Mt weapon (based on a formula that relates this ratio to yield).¹² Later, they refer to both a stem radius and a cloud radius of 2.3 miles.¹³ In any case, their source for the data is *The Effects of Nuclear Weapons*, which gives us yet a third and a fourth story on cloud and stem radius because the version of the book that they used has been superseded by more recent version. In the earlier version (1964, pp. 36-37), the cloud radius for a 1-Mt warhead is given as roughly 10.5 miles, and the ratio of the stem to cloud radius is

¹¹A true window would be a period of time in which no local fratricide would occur. If, however, some could occur, the quality of the window is less than perfect. The higher the probability of fratricide, the lower the quality of the window.

¹²Steinbruner and Garwin, p. 177.

¹³Steinbruner and Garwin, p. 179.

described as: "For yields below about 20 kilotons, the radius of the stem of the mushroom cloud is about half the cloud radius. With increasing yield, however, the ratio of these dimensions decreases, and for yields in the megaton range the stem may be only one-fifth to one-tenth as wide as the cloud." The 1977 version (pp. 32-34) retains this latter comment exactly, but shows the cloud radius at 1 Mt to be about 5.5 miles, or roughly half the size of that in the earlier edition. Therefore, based on this more recent information, a cloud radius of roughly five miles and a stem radius of 0.5 to 1.0 mile is probably appropriate for the fratricide modeling herein, with the 1-mi stem radius probably closer, since 1-Mt warheads are at the bottom of the megaton range. Because Steinbruner and Garwin's article is unclear on this issue, it is not known what effect these values would have, especially on area fratricide.

Steinbruner and Garwin estimate a minimum of five minutes after the burst for the start of the second window, and suggest that six to eight minutes may be more reasonable. This timing is based on the amount of time required for lethal-size debris particles to fall out of the cloud, where the lethal size is assumed to be 10 grams.¹⁴ It is, however, argued that this particle size may be too large (a smaller size would increase the fall time by about 25 percent, it is suggested), and that cloud stabilization time could also increase this time by adding to the time before which the particle can fall.¹⁵

Using one of the more standard fallout models, SEER, it is possible to estimate this fall time from the perspective of the extensive work which has been done on fallout.¹⁶ To begin with, the cloud from a 1-Mt burst rises to about 65,000 ft (cloud top) by its stabilization time of about 9.2 minutes. From this height, a 7-gram particle (the largest size in SEER) falls to the earth in 13 minutes. Thus, for a 7-gram particle, at least part of the cloud could cause fratricide up to 22.2 minutes after detonation. For a 2.6-gram particle (the smaller lethal size used by Steinbruner and Garwin), this time might extend another couple of minutes. Although some other fallout work indicates that particles as heavy as 10 grams would begin to fall out of the cloud before the full 9-minute stabilization time, it is nonetheless significant to note that the actual start of the second window could be much later than

¹⁴Steinbruner and Garwin, pp. 178-181.

¹⁵Steinbruner and Garwin, p. 180.

¹⁶See Paul W. Wong and Hong Lee, *Utilization of the SEER Fallout Model in a Damage Assessment Computer Program (DACOMP)*, Stanford Research Institute, DNA-3608F, February 1975. The 7-gram particle size used below is calculated from Steinbruner and Garwin's specific density of 2.5 and by assuming that SEER's largest particle size, 8768 microns, is spherical (p. 20). Fall times are on p. A-8 of the SEER manual, cloud stabilization time is given on p. A-23 (as variable TSR), and cloud top height on p. A-22 (variable ATC).

Steinbruner and Garwin indicate; indeed, for some potentially lethal particles, the time could be from 20 to 30 minutes. Naturally, the debris particles will tend to move with prevailing winds as they fall, both dispersing and moving away from the initial detonation point. Also, assuming that the nuclear cloud should be wider (5.5 miles versus 2.3) than Steinbruner and Garwin indicate, leakage of warheads through that cloud, rather than complete loss to fratricide, could well occur between the two windows.

TRYING TO OVERCOME FRATRICIDE

Besides control of timing, there are at least two other ways in which an attacker could attempt to overcome fratricide. One is to pattern-bomb the target to move the lethal fratricide effects of earlier warheads away from their successors. The other is to airburst at least the first warhead assigned to a target in an attempt to limit the amount and size of debris produced. The above data tend to indicate that the first just is not very practical: a stem size of one mile would require a separation of one mile between warheads for the later ones to survive with confidence, but such a separation would move the other warheads so far away from a 2000 psi target that they would not damage it. Patterns of a more reasonable size (say 600 ft) would cause the second and subsequent warheads to fly through almost as much of the cloud stem as if no pattern were used, and thus would not lead to a substantial improvement in survival from fratricide. Indeed, a stem size of one-half to one mile would justify the trench fratricide estimate shown in Fig. 43 in R-2577-FF.

On the other hand, an airburst of at least the first warhead assigned to a target could indeed decrease the possibility of fratricide for later warheads. In particular, most of the debris particles of a lethal size drawn into the cloud come from the crater created by a surface burst.¹⁷ *The Effects of Nuclear Weapons* indicates that above a scaled height of burst of 20 to 30 ft (200 to 300 ft for a 1-Mt warhead), not much of a crater forms.¹⁸ Similarly, in the SEER fallout model, the 1000-ft height of burst nominally assumed in the text for a 1-Mt warhead would fail to produce debris particles larger than about 40 to 50 microns in radius, which would be perhaps one-millionth the lethal weight assumed by Steinbruner and Garwin. Therefore, at least according to the fratricide mechanism used by Steinbruner and Garwin, airbursts like those suggested here would probably not cause

¹⁷Norment et al., p. 18.

¹⁸Glasstone and Dolan, pp. 255-256.

much fratricide later than the initial few seconds after a warhead detonates, strongly supporting the value of using airbursts for the earlier warhead(s) assigned to a target. The fratricide model used in the text does not explicitly recognize this possibility, and therefore oversimplifies the calculation (and may overestimate ICBM survivability as well).

Appendix F

CONFIDENCE IN OVERCOMING MPS DECEPTION

In Sec. V of R-2577-FF, an attack multiplier for MPS (Multiple Protective Shelter) systems was introduced. One of the terms in the attack multiplier is E, the percentage of specific shelters in the MPS system which the attacker could identify as empty (i.e., containing no missiles). The attack multiplier formulation assumes that the attacker is *absolutely sure* that all shelters in this fraction of the MPS system are empty. However, for either shelters or trenches, it is unlikely that the attacker will ever be that confident. Instead, he will have some information on differential rates of visit or some such observables upon which he may conclude with a relative probability that some percentage of the MPS system is less likely to have a missile in any given shelter. This appendix assesses the implications of less than perfect certainty that a part of the MPS system is, indeed, empty.¹

THE BASIC FORMULATION

We begin by assuming an MPS system with N missiles (nominally 300) and D shelters per missile (nominally 20). By some form of intelligence gathering, the attacker is able to determine that a given subset of shelters has a relatively low probability of containing a missile. The fraction of all shelters represented by this subset will be referred to as L (the low probability subset fraction); the fraction of shelters not included in this subset will be referred to as H (the high probability subset fraction).² Since all shelters fit into one of these two categories,

$$L + H = 1 \quad (1)$$

If the attacker is unable to establish a low probability subset ($H = 1$), then he must assume that each shelter is equally likely to contain

¹To simplify terminology, this appendix refers to deception in a shelter system, although this analysis can be generalized to any type of MPS system.

²Normally, the probability of finding a missile in any one of these high probability shelters will still be quite low, although higher than the probability of finding a missile in any given low probability shelter.

a missile. Thus, the probability that a missile is in any given ("high probability") shelter is the number of missiles divided by the total number of shelters, or

$$P_H = \frac{N}{N \cdot D} \quad \text{for } L = 0$$

$$= \frac{1}{D} \quad (2)$$

For the nominal example, the attacker would have a 5 percent probability of finding the missile in any given shelter.

If, however, the attacker is able to separate out a low probability subset, he can then determine the relative probability of a missile being in the high versus the low probability subsets of shelters. By implication,

$$P_H > P_L \quad \text{for } L \neq 0 \quad (3)$$

where P_L is the probability that a missile is in any given low probability shelter. If the high probability shelters contain N_H missiles, then

$$N_L + N_H = N \quad (4)$$

Further, P_L and P_H can be calculated from³

$$P_L = \frac{N_L}{L \cdot N \cdot D} \quad (5)$$

$$P_H = \frac{N_H}{H \cdot N \cdot D} \quad (6)$$

Substituting Eqs. (5) and (6) into Eq. (4) for N_L and N_H gives

$$P_L \cdot L \cdot N \cdot D + P_H \cdot H \cdot N \cdot D = N$$

$$\text{or} \quad P_L \cdot L + P_H \cdot H = \frac{1}{D} \quad (7)$$

Using Eqs. (7) and (3) together shows that

³We assume here and throughout this appendix that the attacker has properly assessed the relative distribution of missiles between these two subsets.

$$P_H > \frac{1}{D} > P_L \quad \text{for } L \neq 0 \quad (8)$$

If, for example, 20 percent of the shelters were considered low probability ($L = 0.2$, $H = 0.8$), and only 10 percent of the missiles were in those shelters ($N_L = 30$, $N_H = 270$), then from Eqs. (5) and (6):

$$\begin{aligned} P_L &= \frac{30}{0.2 \cdot 300 \cdot 20} & P_H &= \frac{270}{0.8 \cdot 300 \cdot 20} \\ &= \frac{30}{1200} & &= \frac{270}{4800} \\ &= 0.025 & &= 0.05625 \end{aligned}$$

The ability of the attacker to be relatively more confident of finding a missile in any given shelter of the high probability subset is equal to the ratio of these two probabilities. Defined as confidence (C), this is expressed as

$$C = \frac{P_H}{P_L} \quad (9)$$

For the above example, $C = 2.25$, or a high probability shelter is 2.25 times as likely to contain a missile as a low probability shelter. In the case of perfect confidence, as required of empty shelters in the attack multiplier formulation, C approaches infinity. In a more practical world, C will probably be a much smaller number (though greater than 1, as required by Eqs. (9) and (3)), determined by such evidence as visit rates at certain shelters.⁴

ATTACKING THE MPS SYSTEM

In a world of perfect confidence, an attacker can concentrate his attack on the high probability shelters only, since no missiles are in the low probability shelters. If the kill probability against this subset is PT , then the resulting number of surviving missiles would be

⁴If, for example, security teams were sent to some shelters (to check "intrusions") twice as often as they were sent to other shelters, then the first group would be the high probability subset, and C would equal 2 (as long as security team visits reflect missile location).

$$N_S = N \cdot (1 - PT) \quad \text{for } C = \infty \quad (10)$$

However, in a world with less than full confidence, this same attack would have a different number of survivors:

$$N_S = N_L + N_H \cdot (1 - PT) \quad \text{for } C < \infty \quad (11)$$

Thus, N_L must be kept quite low for the assumption of perfect confidence to be approximately correct.

To understand how N_L relates to confidence, we begin with Eq. (9):

$$C = \frac{P_H}{P_L}$$

We then use Eqs. (5) and (6) for P_L and P_H :

$$\begin{aligned} C &= \frac{\frac{N_H}{H \cdot N \cdot D}}{\frac{N_L}{L \cdot N \cdot D}} \\ &= \frac{N_H \cdot L}{N_L \cdot H} \end{aligned} \quad (12)$$

That is, for a fixed value of N_L (and thus of N_H), confidence must increase dramatically as the percentage of low probability shelters (L) increases (and thus H decreases). This point is illustrated in Fig. F.1, where, for any fixed value of confidence, N_L increases as L increases, making it possible to increase the number of surviving missiles (Eq. (11)) even though the comparable attack multiplier would predict that this number would decrease. Figure 11 also shows that C must increase by an order of magnitude (actually a factor of 11) to reduce N_L from 30 to 3 at any given value of L .

From Eq. (11), the other factor which changes with L is PT , the probability of killing high probability shelters. To understand this point, let TN equal the number of attacking warheads (which we will assume is less than the number of shelters to be attacked), and define Q as the percentage of all shelters that can be struck, or

$$Q = \frac{TN}{N \cdot D} \quad (13)$$

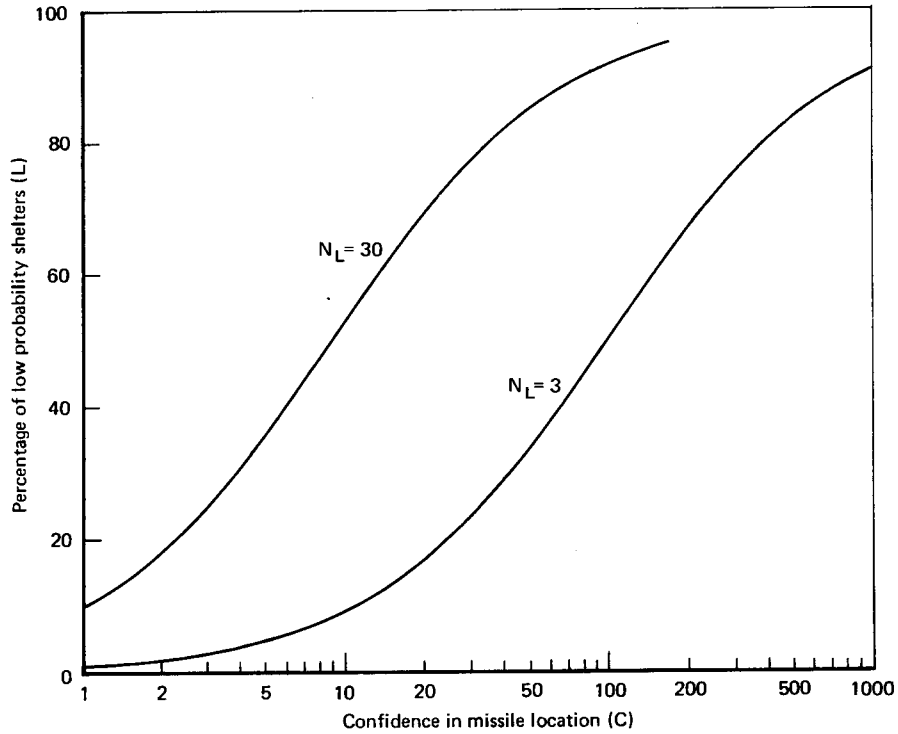


Fig. F.1—Confidence required to guarantee that only a given number of missiles are in low probability shelters

If L equals zero, then PT equals the fraction of the silos attacked times the kill probability of a single warhead against a silo (PK_1), or

$$PT = Q \cdot PK_1 \quad \text{for } L = 0 \quad (14)$$

If, instead, L is greater than zero, then PT can become somewhat more complicated. If H is greater than Q (more high probability shelters than attacking warheads), the attacker would place each warhead on a single high probability shelter, such that PT against the high probability shelters becomes

$$PT = \frac{Q}{H} \cdot PK_1 \quad \text{for } H \geq Q \quad (15)$$

Solving Eq. (12) for N_L and N_H ⁵ and substituting these values into Eq. (11) with the information of Eq. (15) gives

$$\begin{aligned}
 N_S &= \frac{N \cdot L}{C \cdot H + L} + \frac{N \cdot C \cdot H}{C \cdot H + L} \cdot \left(1 - \frac{Q}{H} PK_1\right) \\
 &= \frac{N}{C \cdot H + L} (L + C \cdot H - C \cdot Q \cdot PK_1) \\
 &= N - N \cdot \frac{C \cdot Q \cdot PK_1}{C \cdot H + L} \quad \text{For } H \geq Q \quad (16)
 \end{aligned}$$

For a constant value of confidence within this range ($H \geq Q$), the denominator ($C \cdot H + L$) will decrease as L increases, decreasing the number of surviving missiles (because the denominator will be larger than the numerator if $H \geq Q$). That is, the attacker will minimize the number of surviving missiles within this range if he can decrease the number of high probability shelters to equal the number of attacking warheads while maintaining a constant confidence in missile location.

For attack sizes greater than the number of high probability shelters, the attacker will place a single warhead on each high probability shelter, and will then place the remaining warheads on either some low probability shelters or as a second warhead (with combined kill probability PK_2) on the high probability shelters, depending upon which offers the greater return. Table F.1 summarizes the relevant equations, assuming that two warheads at most would be assigned to each high probability shelter. The variables PT_H and PT_L stand for the kill probability against high probability and low probability shelters, respectively. To see how changes in the number of survivors (N_s) is affected by changes in L , the sign of the derivative $\partial N_s / \partial L$ is given, showing a remarkable degree of continuity across the appropriate

⁵From Eqs. (12) and (4):

$$\begin{aligned}
 N_L &= \frac{N \cdot L}{C \cdot H + L} \\
 N_H &= \frac{N \cdot C \cdot H}{C \cdot H + L}
 \end{aligned}$$

Table F.1
EQUATIONS FOR DETERMINING THE NUMBER OF SURVIVING SHELTERS

Param- eter	H < Q			
	Strike high probability shelters twice, then low probability shelters		Strike high probability shelters twice, then low probability shelters	
	Warheads assigned to high probability shelters only, H ≥ Q	Strike high probability shelters first, then low probability shelters	Warheads assigned to high probability shelters only, some receive two warheads, 2 · H ≥ Q	Two warheads assigned to high probability shelters, 2 · H < Q
PT _H	$\frac{Q \cdot PK_1}{H}$	PK ₁	$\frac{Q - H}{H} \cdot PK_2 + \frac{2 \cdot H - Q}{H} \cdot PK_1$	PK ₂
PT _L	0	$\frac{Q - H}{L} \cdot PK_1$	0	$\frac{Q - 2 \cdot H}{L} \cdot PK_1$
N _S	$N \left[1 - PK_1 \cdot \frac{C \cdot Q}{C \cdot H + L} \right] N \left[1 - PK_1 \cdot \left(1 - \frac{1 - Q}{C \cdot H + L} \right) \right]$	$N \left[1 - PK_1 \cdot \left(1 - \frac{1 - Q}{C \cdot H + L} \right) \right]$	$N \left[1 - \frac{PK_2 \cdot (Q - H) \cdot C + PK_1 \cdot (2 \cdot H - Q) \cdot C}{C \cdot H + L} \right]$	$N \left[1 - \frac{PK_2 \cdot C \cdot H + PK_1 \cdot (Q - 2 \cdot H)}{C \cdot H + L} \right]$
$\frac{\partial N_S}{\partial L}$	+	-	$- : C < 1 + \frac{2 \cdot PK_1 - PK_2}{Q \cdot (PK_2 - PK_1)}$ $+ : C > 1 + \frac{2 \cdot PK_1 - PK_2}{Q \cdot (PK_2 - PK_1)}$	- ^a
C _D	$\frac{PD \cdot L}{Q \cdot PK_1 - PD \cdot H}$	$1 + \frac{PD - Q \cdot PK_1}{H \cdot (PK_1 - PD)}$	$\frac{PD \cdot L}{(Q - H) \cdot PK_2 + (2 \cdot H - Q) \cdot PK_1 - PD \cdot H}$	$\frac{PD \cdot L - (Q - 2 \cdot H) \cdot PK_1}{H \cdot (PK_2 - PD)}$

^aActually, the derivative here would be positive if $C < \frac{(2 - Q) \cdot PK_1}{PK_2 - Q \cdot PK_1}$. However, for these values of C, this procedure is never optimal (one warhead on high and low probability shelters is better) as long as $Q \leq 1$.

regions. Finally, C_D indicates the level of confidence required to obtain a desired level of damage (PD) to the MPS-based missiles.

To make these equations more understandable, they are applied to the nominal attack data in Table F.2. To produce this table, the value of the attack size (Q) was assumed to be 0.7 (4200 warheads divided by 6000 shelters), the number of missiles (N) was taken as 300, and the two kill probabilities PK_1 and PK_2 were assumed to be 0.882 and 0.978, respectively. For attacks where H is greater than or equal to the attack size ($Q = 0.7$), the first column indicates the relevant formulas. For smaller values of H , the attacker must choose a strategy. After he covers the high probability shelters first, he must then decide where to target his extra warheads. If he is very certain that the high probability shelters contain most of the missiles, then he is better off to allocate the extra warheads to the high probability shelters (using the formulas of columns 3 or 4, as opposed to column 2 in Table F.2). This condition will be met if

$$C \geq \frac{PK_1}{PK_2 - PK_1} \quad (17)$$

For our example, this value of C is about 9.2. Figure F.2 demonstrates the combinations of C and L for which the various equations apply.

Figure F.3 demonstrates, for the nominal case, the combinations of L and C that lead to four different numbers of missiles surviving. At a fixed value of L (especially around 50 percent or above), increasing the confidence of locating missiles in the high probability shelters can significantly decrease the number of survivors. On the other hand, reducing the number of high probability shelters at a constant level of confidence does not necessarily lead to any fixed change in surviving missiles. Instead, because of discontinuities in the warhead allocation functions, optimal values for L exist at the functional boundaries. That is, any given number of survivors can be obtained with a minimum requirement of confidence at one of these boundaries (e.g., $H = Q$ or $H = Q/2$). Therefore, the attacker will generally maximize his attack effectiveness if he sizes his intelligence collection process to his nominal attack size, or vice versa. This conclusion assumes that the attacker is able to maintain the same level of confidence (C) at differing levels of high probability and low probability shelters, an assumption that may well depend heavily on how the United States maintains deception. On the other hand, beyond these

Table F.2
NOMINAL FORMULATION OF SURVIVING SHELTERS

Param- eter	H < .7		
	H ≥ .7	No more than one warhead per shelter	Two warheads on high probability shelters
			.7 > H ≥ .35 H < .35
P _T H	$\frac{.62}{H}$.88	$.78 + \frac{.07}{H}$.98
P _T L	0	$.88 - \frac{.26}{L}$	0 $1.76 - \frac{1.15}{L}$
N _S	$300 \cdot \left[1 - \frac{.62 \cdot C}{C \cdot H + L} \right]$	$300 \cdot \left[.12 + \frac{.26}{C \cdot H + L} \right]$	$300 \left[1 - C \cdot \frac{.78 \cdot H + .07}{C \cdot H + L} \right]$ $300 \left[\frac{.98 \cdot C \cdot H + 1.76 \cdot L - 1.15}{C \cdot H + L} \right]$
$\frac{\partial N_S}{\partial L}$	+	-	- : C < 12.7 + : C > 12.7
C _D	$\frac{PD \cdot L}{.62 - PD \cdot H}$	$1 + \frac{PD}{H} - \frac{.62}{(.88 - PD)}$	$\frac{PD \cdot L}{.78 \cdot H + .07 - PD \cdot H}$ $\frac{PD \cdot L - 1.76 \cdot L + 1.15}{H \cdot (.98 - PD)}$

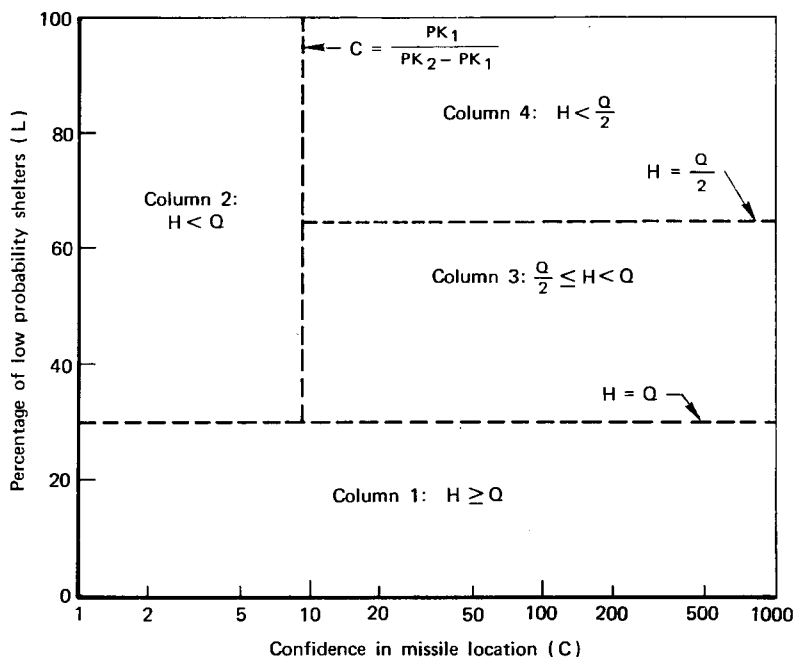


Fig. F.2—Areas of “deception space” where the different formulations apply

two optimal points, the attacker has little incentive to increase the

The two optimal points for overcoming deception change significantly with attack size, as shown in Fig. F.4 for the nominal data and 60 surviving missiles (N_s). For large attack sizes, relatively little confidence in actual missile location is required, especially for the indicated value of N_s . As the attack becomes smaller, both the percentage of low probability shelters and the confidence in missile location must increase significantly to maintain a fixed number of survivors. Still, the attacker would require only 600 warheads (or less) to accomplish this task if he can make the percentage of high probability shelters low enough and his confidence in missile location high enough.

⁶This statement assumes that at most two warheads would be assigned to each high probability shelter. If three could be assigned, a third optimal point would exist at $H = Q/3$, and so forth with more warheads assigned.

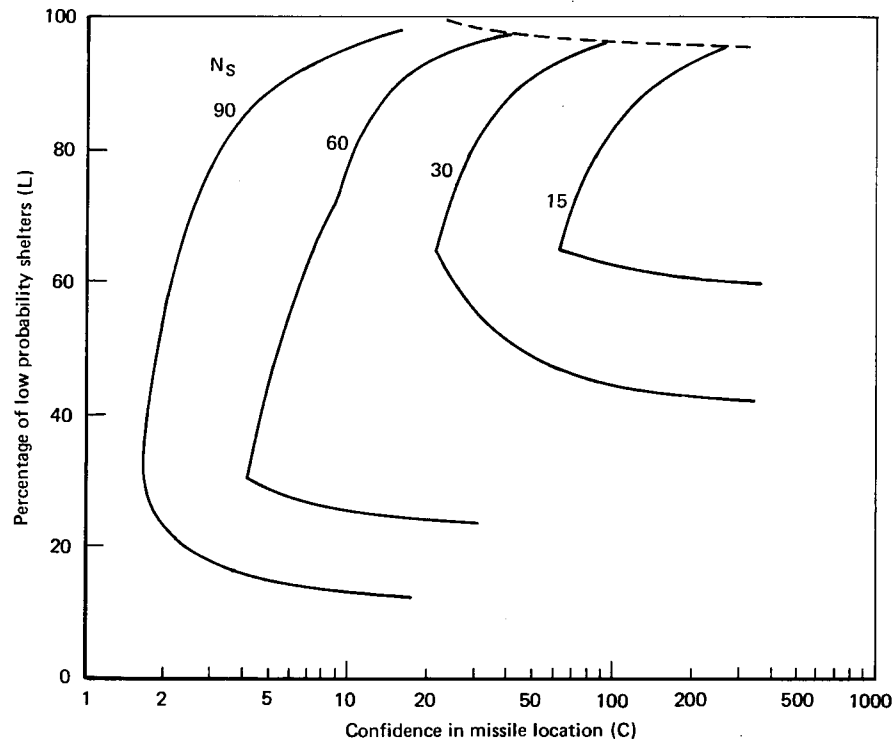


Fig. F.3—Breakdown in deception required for specific number of surviving missiles (N_S)

THE LIMITS OF CONFIDENCE

If the attacker were able to reduce the fraction of high probability shelters to a small percentage, the formulation would encounter a potential flaw: extremely high confidence (C) values can, mathematically, imply that more missiles are in high probability shelters than there are such shelters. To overcome this problem, a limitation must be enforced:

$$N_H \leq H \cdot N \cdot D$$

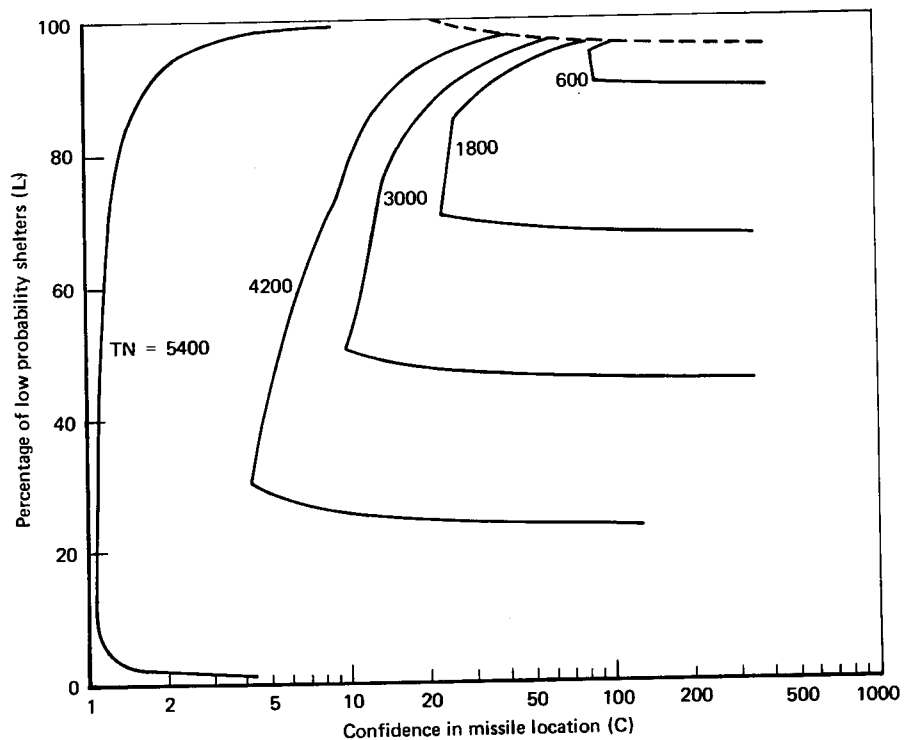


Fig. F.4—Breakdown in deception required for different force sizes to reduce the number of surviving missiles to 60

Combining this equation with Eqs. (12) and (4) yields

$$\frac{N \cdot C \cdot H}{C \cdot H + L} \leq H \cdot N \cdot D$$

$$C \leq D \cdot C \cdot H + L \cdot D$$

$$C \left(\frac{1}{D} - H \right) \leq L$$

$$C \leq \frac{L}{\frac{1}{D} - H} \quad (18)$$

Note that the last transformation is only true if

$$\frac{1}{D} > H$$

In other words, problems will develop only if the percentage of high probability shelters is less than the percentage of shelters which *really do* have missiles in them. The dashed lines in Figs. F.3 and F.4 show the area where the confidence formulation has this problem for the nominal assumptions, and therefore confidence levels that never can be obtained for the given percentage of high probability shelters.

CONCLUSIONS

For an MPS system to work, the defender must prevent the attacker from gaining any significant amount of confidence about the actual location of the defender's missiles. As both Figs. F.3 and F.4 show, even a little bit of information of this sort can help the attacker; on the other hand, these figures also show that the attacker must be very certain about the location of the missiles before he can reap the benefits shown by the deception multiplier in the text.

Also, these calculations assume that the attacker is correct in his estimates about where the missiles really are; if he is not, his attack would probably yield a lower kill probability (though he could also get a higher kill probability in some cases). However, since all of these factors are relatively complicated, the more simple deception multiplier is used in R-2577-FF, recognizing that it tends to overstate true kill probability and understate the uncertainties.

BIBLIOGRAPHY

- Analyses of Effects of Limited Nuclear Warfare*, Subcommittee on Arms Control, International Organizations and Security Agreements of the Committee on Foreign Relations, United States Senate, September 1975.
- Ballistic Missile Staff Course Study Guide*, 4315 Combat Crew Training Squadron, Vandenberg Air Force Base, California, May 1, 1978.
- Bennett, Bruce, *Fatality Uncertainties in Limited Nuclear War*, The Rand Corporation, R-2218-AF, November 1977.
- Brode, H. L., and J. G. Lewis, "Implications of Recent Airblast Studies to Damage of Hardened Structures," in W. J. Hall (ed.), *Structural and Geotechnical Mechanics*, Prentice-Hall, Inc., Englewood Cliffs, New Jersey, 1975, pp. 55-69.
- Counterforce Issues for the U.S. Strategic Nuclear Forces*, Congress of the United States, Congressional Budget Office, January 1978.
- DIA, *Mathematical Background and Programming Aids for the Physical Vulnerability System for Nuclear Weapons*, DI-550-27-74, November 1, 1974, with Change 1 (August 1, 1976).
- Glasstone, Samuel, and Philip J. Dolan (eds.), *The Effects of Nuclear Weapons*, U.S. Department of Defense and U.S. Department of Energy, 1977.
- Norment, H. G., W.Y.G. Ing, and J. Zuckerman, *Department of Defense Land Fallout Prediction System*, Vol. II: *Initial Conditions*, Technical Operations Research, DASA-1800-2, September 1966.
- Robinson, Clarence A., Jr., "U.S. Weighs New SALT Offer to Soviets," *Aviation Week and Space Technology*, September 4, 1978, pp. 24-26.
- Steinbruner, John, and Thomas Garwin, "Strategic Vulnerability: The Balance Between Prudence and Paranoia," *International Security*, Summer, 1976.
- Tsipis, Kosta, *Nuclear Explosion Effects on Missile Silos*, Center for International Studies, Massachusetts Institute of Technology, February 1978.
- Wong, Paul W., and Hong Lee, *Utilization of the SEER Fallout Model in a Damage Assessment Computer Program (DACOMP)*, Stanford Research Institute, Stanford, California, DNA-3608F, February 1975.

RAND/R-2578-FF